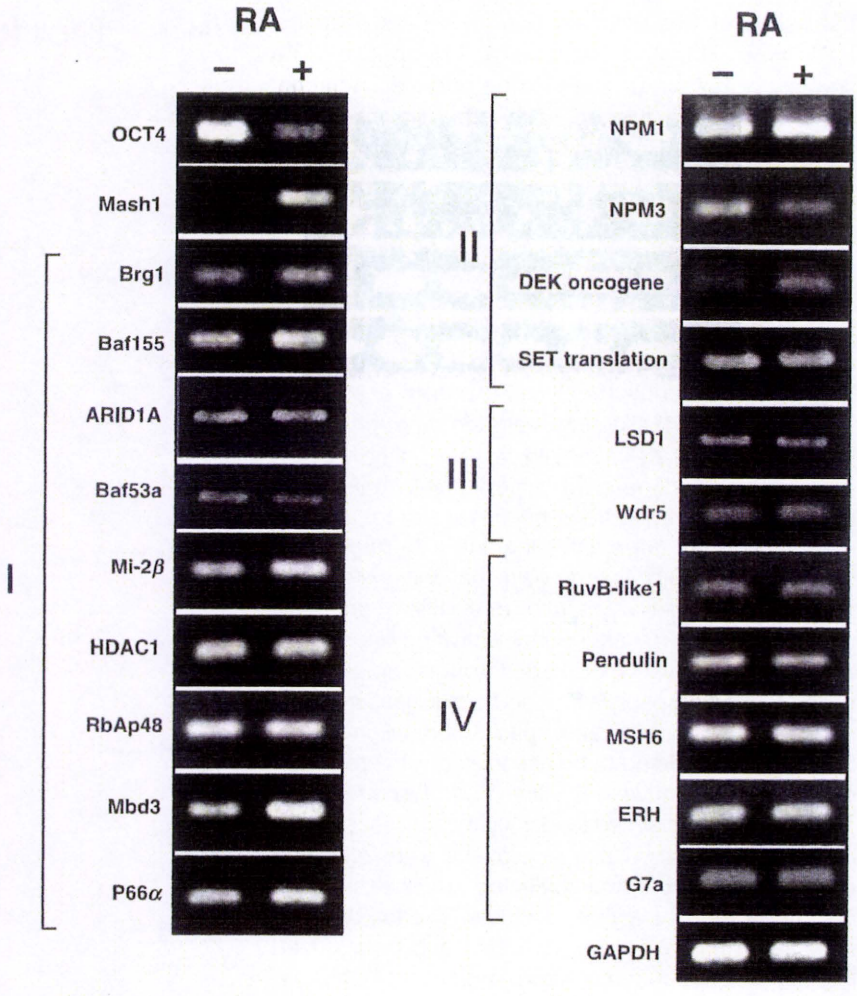

Fig. 2. Gene expression levels of histone tail-associated proteins in the undifferentiated and the differentiated embryonic stem (ES) cells. D3-ES cells were cultured for 120 h in the absence (−) and presence (+) of 0.5 μM retinoic acid (RA). RNA was extracted from both states of cells for semiquantitative reverse transcription–polymerase chain reaction (RT–PCR) to measure the expression levels of the indicated 20 genes. GAPDH (glyceraldehyde 3-phosphate dehydrogenase) gene was used as an internal control gene. The Roman numerals I to IV represent categories of nuclear proteins: I, chromatin remodeling proteins; II, histone chaperones; III, histone modification-related proteins; and IV, others. The experiments were independently carried out twice and similar results were obtained. A result of the two experiments is presented here. Similar results were also obtained from the experiment with CMT-1-ES cells.

and which preserve their original pluripotency in that they can be used for germ-line transmission when used according to the manufacturer's instructions (Cell & Molecular Technologies, New Jersey, NJ, USA), and D3-ES cells (ATCC, Manassas, VA, USA). These two types of ES cell are of the same origin (129/SV strain). We used CMT-1-ES cells for short-term culture experiments (up to 2 days; Figs 1 and 4A) in the presence of fetal bovine serum (FBS). D3-ES cells were used for long-term culture experiments (3–5 days, Figs 2 and 3), in which ES cells were characterized in terms of undifferentiated (RA-untreated) and differentiated (RA-treated) states. These cells were also used in experiments, in which the effect of NPM3 on the undifferentiated ES cells was examined in a long-term culture (3 days, Fig. 5). CMT-1-ES cells were cultured in high glucose Dulbecco's Modified Eagle Medium (DMEM) supplemented with 10% FBS and 1000 IU/mL LIF provided by Cell & Molecular Technologies on 0.1% gelatin-coated dishes. D3-ES cells were cultured on 0.1% gelatin-coated dishes in Glasgow's MEM (GMEM) supplemented with 10% KnockOut serum replacement (Invitrogen, Carlsbad, CA, USA), 1 × nonessential amino acids (Invitrogen), 1 mM sodium pyruvate, 0.1 mM β-mercaptoethanol (Sigma, St. Louis, MO, USA), 1000 IU/mL ESGRO (Invitrogen), and 1 μM ACTH (American Peptide Company, Sunnyvale, CA, USA; Ogawa *et al.* 2004). We confirmed that both types of ES cells showed similar characteristics in their expression profiles of mRNA and proteins, and the effects of RA on their expression (data not shown). Thus, ES cells are described simply as ES cells without referring to the original name of the cell lines (CMT-1 or D3) unless specified. Both types of ES cells were at 11 passages when purchased. ES cells were maintained without feeder cells and were used within four passage numbers. To obtain differentiated ES cells, D3-ES cells were cultured for up to 120 h in the presence of 0.5 μM RA (Sigma), under which ES cells are known to differentiate into neural

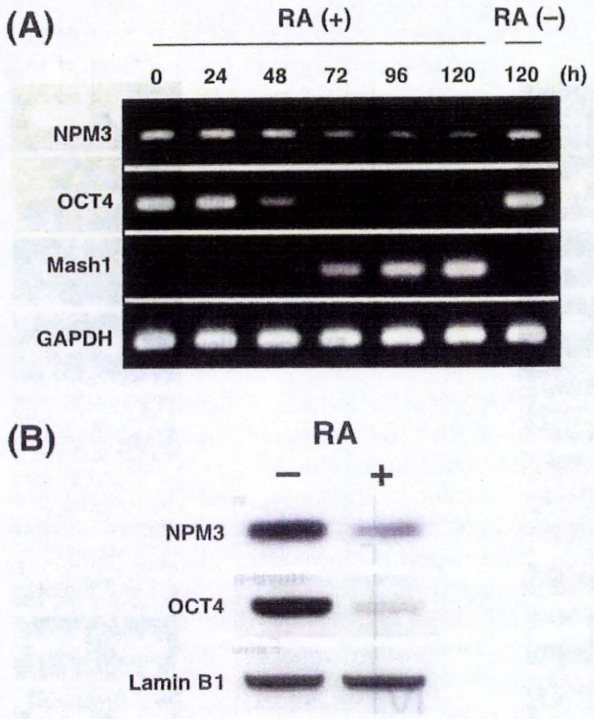

Fig. 3. Expression levels of nucleoplasmin 3 (NPM3) mRNA and protein during retinoic acid (RA)-induced differentiation. (A) mRNA expression. D3-ES cells were treated with 0.5 μM RA for up to 120 h and total RNA was isolated at the indicated time points for semiquantitative reverse transcription–polymerase chain reaction (RT–PCR) to estimate mRNA levels of NPM3, OCT4, and Mash1. GAPDH gene was used as an internal control gene. Similar results were also obtained from the experiment with CMT-1 cells. (B) Protein expression. D3-ES cells were cultured for 120 h in the absence (–) and presence (+) of 0.5 μM RA. Whole cell lysates were prepared for Western blotting of NPM3 and OCT4, and Lamin B1 as an internal control. Similar results were obtained from the experiment with CMT-1-ES cells.

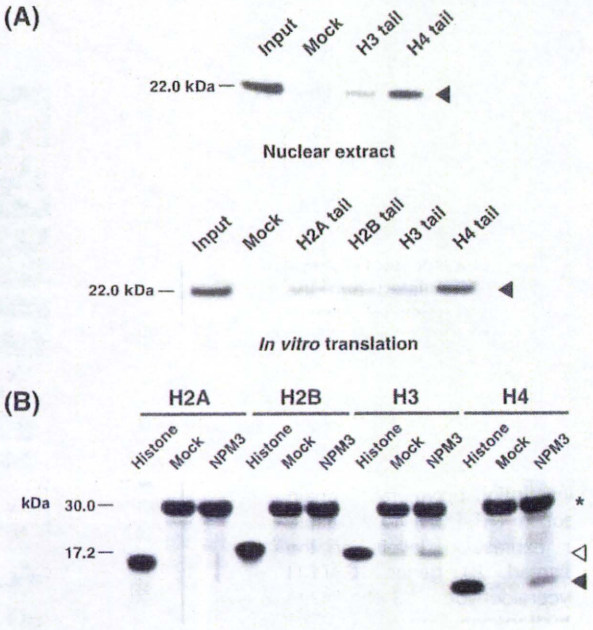

Fig. 4. Specificity of nucleoplasmin 3 (NPM3) binding to histone tails. (A) NPM3 binding to the tail domains of core histones. Upper panel. Nuclear extracts of CMT-1-ES cells were incubated with the beads bearing each of the tail peptides of histone H3 and H4. The proteins bound to the beads were subjected to Western blotting for NPM3. Lower panel. *In vitro* synthesized NPM3 was incubated with the beads bearing each of the tail peptides of H2A, H2B, H3, and H4. The proteins bound to the beads were processed as in the upper panel. 'Input' represents a Western blot of NPM3 in which the same amount of NPM3 as in the binding experiments was directly loaded on sodium dodecyl sulfate–polyacrylamide gel electrophoresis (SDS–PAGE) gels without incubation with beads. 'Mock' represents samples incubated with streptavidin-agarose beads that did not bind the tail peptides. The arrowhead at the right side of the gel points to NPM3 bands. The positions of the molecular mass (22.0 kDa) of NPM3 in kDa are indicated at the left side of the panel. (B) Binding of NPM3 with histone H2A, H2B, H3, and H4. Four types of histone each were incubated with anti-Flag M2 agarose beads on which *in vitro* synthesized Flag/NPM3 had been immobilized. The bound histones were separated by 4–12% gradient SDS–PAGE gels and visualized by CBB R-250. 'Mock' represents each histone incubated with anti-Flag M2 agarose beads that did not bind NPM3. 'Histone' indicates each calf thymus histone as loading markers. The asterisk at the right side of the gel points to immunoglobulin G (IgG) light chain bands that originated from anti-Flag IgG. The white and black arrowheads at the right side indicate the locations of histones H3 and H4, respectively. The positions of molecular mass markers in kDa are indicated at the left side of the panel. The graphs in A and B represent the results of one of the two independent experiments, which each showed similar results to the other.

precursor cells (Lee *et al.* 1994). LIF was removed from the culture media when cells were treated with RA.

Protein extraction and pull-down assay

Nuclear extracts of ES cells were obtained using a Nuclear Extraction Kit (Active Motif, Carlsbad CA, USA) according to the supplier's protocol. The 21-amino acid residue-long peptides (1–21 aa) starting from the N-terminus of the tail domain of histone H3 and H4 were purchased from Upstate (Charlottesville, MA, USA), which were biotinylated at the C-terminus. The peptides, 20 μg each, were incubated for 12 h at 4°C with 50 μL streptavidin-agarose beads included in a Pro-bound biotinylated pull-down kit (Pierce, Rockford, IL, USA). Nuclear extracts were dialyzed against phosphate-buffered saline (PBS) containing a complete ethylenediaminetetraacetic acid (EDTA)-free protease inhibitor cocktail (Roche, Basel, Switzerland) for 12 h at 4°C and diluted with PBS to a final protein concentration of 1 mg/mL. The extracts, 500 μL each, were incubated with the peptide-linked streptavidin beads

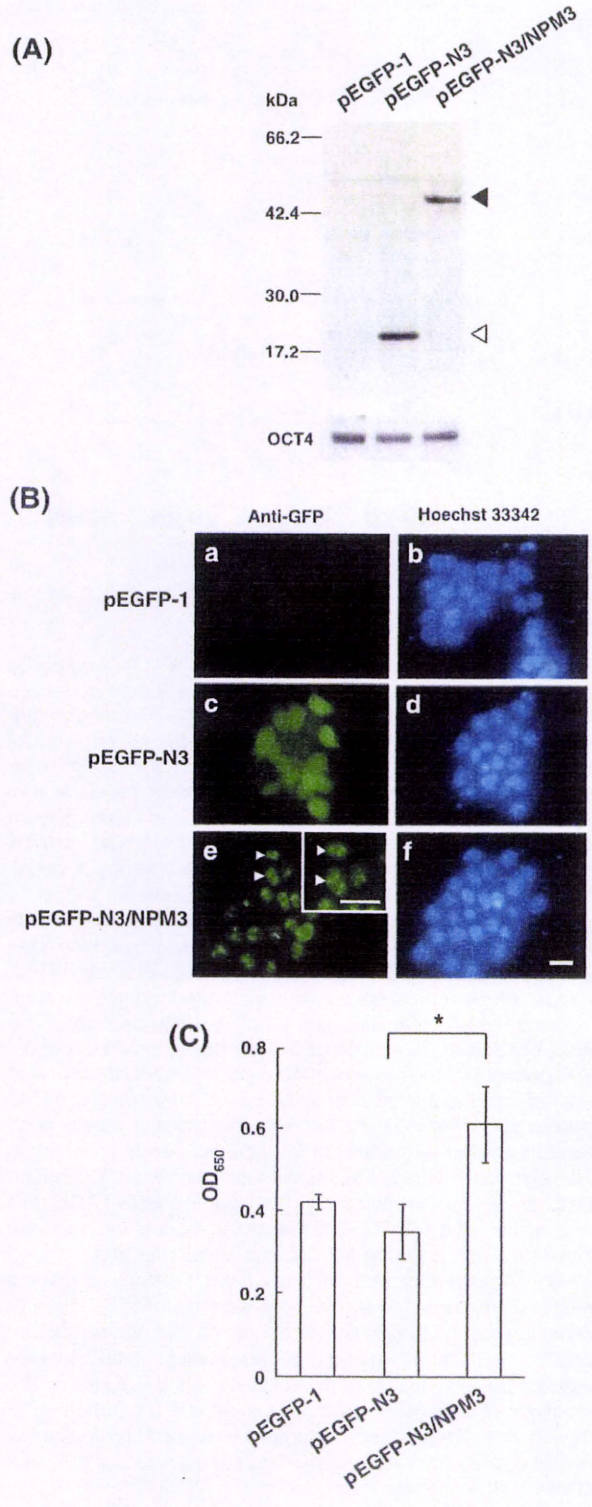

Fig. 5. Enhanced proliferation of nucleoplasmin 3 (NPM3)-overexpressing embryonic stem (ES) cells. D3-ES cells were transfected with each of pEGFP-1, pEGFP-N3, and pEGFP-N3/NPM3. (A) Western blot analysis of enhanced green fluorescent protein (EGFP)/NPM3 in transfected ES cells. Cell lysates were prepared from the transfected cells and subjected to Western blot analysis with anti-GFP antisera and with anti-OCT4 antibodies for checking the equal loading. The upper closed and lower open arrowhead at the right side point to the positions corresponding to the molecular masses of EGFP/NPM3 and EGFP proteins, respectively. The positions of molecular mass markers in kDa are indicated at the left side of the panel. (B) Localization of EGFP/NPM3 in ES cells. The transfected ES cells were subjected to immunocytochemistry using anti-GFP antibodies (a, c, e) and to Hoechst 33342 nuclear staining (b, d, f). EGFP/NPM3 proteins were localized in nucleoli (arrowheads in e), whereas EGFP protein was diffused in cytoplasm. The inset in e a magnified photo of a region including the cells indicated by arrowheads. Bar, 20 μm (C) Proliferation of the transfected cells. ES cells, 2×10^4 cells each, were placed in 96-well plates and transfected with pEGFP-1, pEGFP-N3, and pEGFP-N3/NPM3. The ES cells were allowed to proliferate for 3 days post-transfection and processed for 3-(4, 5-dimethylthiazolyl-2)-2, 5-diphenyltetrazolium bromide (MTT) assay. Student's *t*-test was used for statistical analysis for pEGFP-N3 vs. pEGFP-N3/NPM3. $^*P < 0.01$. The experiments of A through C were independently carried out three times, and each showed similar results to the others. The graphs in A and B represent the results of the three experiments.

for 12 h at 4°C. After washing with Tris-buffered saline (TBS), the beads were eluted by glycine-buffer (pH 3.0). The eluates were concentrated using a Biomax MW 5000 column (Millipore, Billerica, MA, USA), separated by 4–12% gradient NuPAGE (Invitrogen), and were visualized by Coomassie Brilliant Blue (CBB) R-250. CBB R-250 stained bands were cut off and trypsinized by in-gel digestion, and then the proteins were identified by mass spectrometry according to Yamagata *et al.* (2002).

RT–PCR analysis

Total RNA was extracted from ES cells by an RNeasy mini kit with DNase I-treatment (Qiagen, Valencia, CA, USA) and used to synthesize cDNAs using random hexamers using a Thermoscript kit (Invitrogen). The cDNAs were subjected to semiquantitative reverse transcription–polymerase chain reaction (RT–PCR) analysis using AmpliTaq Gold (Applied Biosystems, Foster City, CA, USA) with the gene-specific primers listed in Table 1. PCR products underwent electrophoresis on 1.5% agarose gels and were visualized by ethidium bromide. The band corresponding to the products of NPM3 gene was quantified using Image J (National Institutes of Health, Bethesda, MD, USA).

Construction of expression vectors and their transfection into ES cells

Fusion cDNA consisting of Flag-tag and the full-length of mouse NPM3 (Flag/NPM3) was amplified by PCR using KOD-Plus-Taq polymerase (TOYOBO, Osaka,

Table 1. List of primers used in reverse transcription–polymerase chain reaction

Gene	Primers	Expected product size (bp)
Mi2β	S: 5′-TGCTGCAACCACCCTTATCTC-3′ AS: 5′-AGTGGCCAGATTGATCCCAAG-3′	360
HDAC	S: 5′-GGCTGGCAAAGGCAAGTACTA-3′ AS: 5′-TTTCGTAAGTCCAGCAGCGAG-3′	302
RbAp48	S: 5′-AGGAGAAGTGAACAGGGCCC-3′ AS: 5′-AGACTCGTGGAGCAGATGCC-3′	352
Mbd3	S: 5′-GATGAATAAGAGTCGCCAGCG-3′ AS: 5′-AGGGTGCTGGTGTGTAGAGCA-3′	351
p66α	S: 5′-CACCCTTGAACCTGACCTAACG-3′ AS: 5′-GCTTTTCAAGAGCGCCTCAGT-3′	358
Brg1	S: 5′-CATCGCGCTCATCACATACCT-3′ AS: 5′-TCCGGTAGCTTGTTCTGCAG T-3′	393
Baf155	S: 5′-AAGGTGATCCAAGTCGCTCAG AS: 5′-ATTGCCATGGGTCGACTCTCT-3′	361
ARID1A	S: 5′-CAGATCAGAGGGCCAACCAT-3′ AS: 5′-CCGGACTTGAGGGACATCAT-3′	433
Baf53a	S: 5′-CAAGGCATTGTGAAATCCCC-3′ AS: 5′-CTTCAGGAATTTTCAGCCGC-3′	352
NPM1	S: 5′-TGGTCTTACGGTTGAAGTGTGG-3′ AS: 5′-CTCTTGACCCTTTGATCTCGGT-3′	380
DEK oncogene	S: 5′-CGTGAACAGCGAACTCGTGA-3′ AS: 5′-TCTTGGTGGTACTGCTGTCTGC-3′	368
SET translation	S: 5′-CATTCTGACGCAGGTGCTGAT-3′ AS: 5′-AGACCTCAAAACAGGGCGACT-3′	381
LSD1	S: 5′-GGTTCAGGTGTTTCTGGCTTG-3′ AS: 5′-GCAGCTGAATGACAACCTCCA-3′	403
Wdr5	S: 5′-CTGCCTG TAATAGTACCCAGCGT-3′ AS: 5′-GTTCTTCCTCTCCAACACTCAGC-3′	359
RuvB like 1	S: 5′-TGTGACCTTGCATGACCTGG-3′ AS: 5′-TGACACAGTTGCCTCGGTTG-3′	302
Pendulin	S: 5′-GCTCCAAGCTACTCAAGCTGCT-3′ AS: 5′-AACAGTGGGTCAATCGCACC-3′	351
MSH6	S: 5′-GGGCTAAGATGGAAGGTTACCC-3′ AS: 5′-AAGCCTCATGCACCTCTGTCTC-3′	351
ERH	S: 5′-GATGAATCCCAACAGCCCTTC-3′ AS: 5′-ACGGTGGCTTCAGAGTGACAA-3′	359
G7a	S: 5′-ACCTATGACCTCCCTACCCCA-3′ AS: 5′-TGGGTTCCATAGGGTGGTCTC-3′	303
NPM3	S: 5′-AACATGCTGTGCCTTACCGAG-3′ AS: 5′-GGAAGGATGCCACACAGCTTA-3′	302
OCT4	S: 5′-CTGAGGGCCAGGCAGGAGCACGAG-3′ AS: 5′-CTGTAGGGAGGGCTTCGGGCACTT-3′	485
Gapdh	S: 5′-GCACAGTCAAGGCCGAGAAT-3′ AS: 5′-GGTCATGAGCCCTTCCACAA-3′	355
Mash1	S: 5′-GGCTCAACTTCAGCGGCTTC-3′ AS: 5′-GTTGGTAAAGTCCAGCAGCTC-3′	350

Vector construction

Primer	Sequence
NPM3-Flag-sense	5′-CGCGGATCCGCGCGGGGCGCTCACGGCCGT-3′
NPM3-Flag-antisense1	5′-GTCCTTGTAATCGCCGCCAGGCCTGCCCCTGTGCTT-3′
NPM3-Flag-antisense2	5′-CTAGTCTAGACTACTTGTCATCGTCGTCCTTGTAATCGCCGCC-3′
EGFP/NPM3-sense	5′-CGGAATTCCGGGGCGCTCACGGCCGTTTC-3′
EGFP/NPM3-antisense	5′-CGGGATCCAGGCCTGCCCCTGTGCTTCTT-3′

AS, antisense primers; S, sense primers.

Japan) and primer sets for Flag-tagged NPM3 (Flag/NPM3) described in Table 1. The PCR products were subcloned into the *Xba*I/BamH I sites in pDH105 vector (Hsu *et al.* 1998), which yielded pDH105-Flag/NPM3. Fusion cDNA consisting of enhanced green fluorescent protein (EGFP) and the full length of mouse NPM3 (EGFP/NPM3) was similarly amplified using EGFP/NPM3 primers described in Table 1. The products were subcloned into the EcoR I/BamH I sites in CMV (cytomegarovirus) minimum promoter-driven pEGFP-N3 vectors (Clontech, Palo Alto, CA, USA).

Embryonic stem cells (2×10^5 cells) in six-well plate were transfected for 24 h with promoter-less pEGFP-1 (Clontech), pEGFP-N3, or pEGFP-N3/NPM3 using Lipofectamine 2000 (Invitrogen). The ES cells were further cultured for 72 h and were harvested for analysis. Proliferation activity of the transfected cells was measured by 3-(4, 5-dimethylthiazolyl-2)-2, 5-diphenyltetrazolium bromide (MTT) assay using a Cell Counting Kit-8 (DOJINDO, Kumamoto, Japan) as changes of the optical density (OD) at the absorption wavelength of 450 nm against 650 nm.

Histone tail- and histone-binding assay for NPM3

The binding activity of NPM3 to histone tails was examined as follows. Mouse Flag/NPM3 was synthesized *in vitro* using a TNT SP6 Coupled Wheat Germ Extract System (Promega, Madison, WI, USA) and pDH105-Flag/NPM3. Biotinylated tail domain peptides of histone H2A (1–21 aa), H2B (1–22 aa), H3 (1–21 aa), and H4 (1–21 aa) were purchased from Upstate and 20 μg each were incubated with 50 μL streptavidin-agarose beads included in a Pro-bound biotinylated pull-down kit (Pierce) for 12 h at 4°C to obtain histone tail peptide-linked streptavidin beads. The streptavidin-agarose beads were incubated with biotin blocking buffer included in a Pierce's kit in control (mock control) experiments. Flag/NPM3 was diluted with TBS containing a complete EDTA-free protease inhibitor cocktail (Roche), 500 μL of which was incubated with the histone tail peptide-linked streptavidin beads for 12 h at 4°C. After being washed with TBS, the beads were treated with 2 × lithium dodecyl sulfate (LDS) sample buffer (Invitrogen) to elute the bound proteins. The eluates were subjected to Western blot analysis.

The binding activity of NPM3 to histones was examined as follows. Calf thymus histone H2A, H2B, H3, and H4 were purchased from Roche. Mouse Flag/NPM3 was diluted with TBS containing the Complete EDTA-free protease inhibitor cocktail (Roche), 500 μL of which was concurrently incubated with 10 μg of each of the histones and anti-Flag M2 agarose beads (Sigma) for 12 h at 4°C ('anti-Flag M2' represents the antibodies that generally recognize Flag-tag linked to proteins). The beads were washed with TBS three times and boiled with 50 μL 2 × LDS sample buffer (Invitrogen). The supernatants containing the bead-bound proteins were separated by 4–12% gradient NuPAGE (Invitrogen), and were stained with CBB R-250.

Western blot analysis for binding of NPM3 to histone tail, histone, and ES cell-lysate

Anti-mouse NPM3 rabbit antiserum was produced with synthetic C-terminal 12-amino acid residue-long peptides of NPM3. We verified the immuno-reactivity and immuno-specificity of the anti-NPM3 antiserum by Western blot analysis using *in vitro* synthesized NPM3 and other non-related proteins as antigens (data not shown). Western blot analysis for NPM3 binding was carried out using this antiserum on samples obtained from histone tail- and histone-binding experiments, and NPM3 gene-transfected ES cell lysates. Samples of the histone tail- and histone-binding experiments described above were separated by 4–12% gradient NuPAGE. NPM3 gene-transfected ES cells (2×10^5 cells) were directly lyzed in 1 × LDS sample buffer and were separated by 10% NuPAGE. These gels were transferred onto iBlot nitrocellulose membranes (Invitrogen). After blocking with 5% non-fat skim milk in TBS containing Tween 20 (TBST) for 1 h, the membranes were incubated with antirabbit NPM3 antiserum (1:1000 diluted), antirabbit GFP antisera (1:5000; Molecular Probes, Eugene, OR, USA), antirabbit OCT4 antibodies (1:1000; Santa Cruz Biotechnology, Santa Cruz, CA, USA) for 1 h at 37°C or overnight at 4°C. After being washed with TBST three times, the membranes were incubated with horseradish peroxidase-conjugated antirabbit IgG (1:1000; GE Healthcare, Buckinghamshire, UK) or horseradish peroxidase-conjugated antimouse IgG (1:1000; Vector Laboratory, Burlingame, CA, USA) for 1 h at 37°C. Signals were detected with ECL Western blotting detection reagents (GE Healthcare).

Immunocytochemistry

The transfected cells were fixed with 4% paraformaldehyde in PBS for 15 min at room temperature, and were permeabilized with 0.25% Triton X-100 in PBS for 10 min at room temperature. Plates were blocked in 5% BSA in PBS for 1 h at room temperature, and were then incubated with 1:750 diluted antimouse GFP antibodies (Chemicon, Temecula, CA, USA) overnight at 4°C. After being washed with PBST, the cells were incubated with 1:1000 diluted antimouse

IgG Alexa 488 (Molecular Probes) for 1 h at 37°C, washed with PBST, and were treated with Hoechest 33342 (Molecular Probes) for 10 min at room temperature for nuclear staining.

Results

Identification of histone tail-associated proteins

Nuclear extracts were prepared from ES cells and subjected to the pull-down assay using synthesized histone H3 and H4 tail peptides as baits. The proteins bound to baits were separated by sodium dodecyl sulfate–polyacrylamide gel electrophoresis (SDS–PAGE) (Fig. 1). Although the overall banding patterns were similar between the two baits, more proteins were bound to the H4 tail. Thus, in the following study, we focused on the H4 tail-associated proteins. Thirty-six bands were clearly discernible on the H4 tail gel and separable from each other, and were thus selected for identification by mass spectrometry. Five bands failed to produce meaningful mass spectra for sequencing. Altogether, we were able to identify 45 proteins from these bands. Twelve bands (numbers 3, 4, 7, 14, 15, 16, 19, 23, 25, 26, 28, and 31) comprised greater than two proteins (Table 2). These proteins were grouped into four categories, chromatin remodeling proteins, histone chaperones, histone modification-related proteins, and others (Table 2). Approximately a quarter of the proteins identified (10 proteins) were components of either of the two chromatin remodeling proteins, BAF (Brahma Associated Factor) complex (Wang *et al.* 1996a, b) that is known to act as a transcriptional activator (Carlson & Laurent 1994) or NuRD (nucleosomal remodeling and histone deacetylase) complex that acts as a transcriptional repressor (Zhang *et al.* 1999). There were five and two histone chaperones and histone modification-related proteins, respectively. The remaining 28 proteins were categorized as 'others'.

mRNA expressions of histone tail-associated proteins in undifferentiated and differentiated ES cells

In order to determine the biological significance of the histone tail-associated proteins, we compared mRNA expression levels of these proteins between undifferentiated (RA-untreated controls) and differentiated ES cells (RA-treated cells). For this purpose we selected 20 proteins from the above 45 proteins listed in Table 1: the nine chromatin remodeling proteins, the four histone chaperones, the two histone modification-related proteins, and the five from the other 28 proteins. 'Similar to BAF57' protein (number 16) in the chromatin remodeling proteins was not examined because of its uncertainty as a BAF member. Nucleolin (C23) (numbers 8–10) in the histone chaperones was omitted because of its ubiquitous expression in a variety of replicating cells (Tuteja & Tuteja 1998). The 24 proteins classified as 'others' were not examined because of their multifunctional or 'house-keeping' nature. The expression level of OCT4 and Mash1 were also determined as markers of undifferentiated and differentiated cells, respectively. Figure 2 shows mRNA expression levels of these 20 genes estimated by semiquantitative RT–PCR. The control ES cells expressed OCT4 at a higher level than the RA-treated cells as expected. The RA-treated ES cells, but not the untreated cells, expressed mRNA of Mash1, indicating that RA-treatment caused the cells to differentiate into neuronal progenitor cells as reported previously (Lee *et al.* 1994). Most of the genes were expressed at similar levels in both states of ES cells, or at higher levels in the RA-treated cells. However, NPM3 gene (protein 32 in Table 2) was exceptional: the expression level of the NPM3 gene was significantly (approximately 2.4-fold) higher in the undifferentiated ES cells than the differentiated cells relative to expression of a housekeeping gene (GAPDH) whose expression was similar in both control and RA-treated cells. The experiments to compare mRNA expression levels between the two types of ES cells were carried out twice and the same results were reproducibly obtained. Similar results were also obtained from the experiment with CMT-1-ES cells. Therefore, we concluded that NPM3 is a histone H4 tail-binding protein in ES cells and is associated with their undifferentiated state.

Expression of NPM3 mRNA and protein in ES cells during RA-induced differentiation

The above results (Fig. 2) suggested that expression of NPM3 is associated with the 'stemness' of ES cells and led us to further characterize the expression and biological role of this gene during RA-induced differentiation. ES cells were cultured for up to 120 h in the presence of 0.5 μM RA and the expression level of NPM3 was determined by semiquantitative RT–PCR together with the expression level of OCT4 and Mash1 gene as in Figure 2 (Fig. 3A). The expression profile of the NPM3 gene was similar to the OCT4 gene, which decreased during RA treatment, but different from that of the Mash1 gene, which was upregulated by RA at 72 h post-treatment, the expression level of which increased continuously thereafter. The NPM3 gene was expressed at a significant level up to 48 h post-treatment, started to decrease at 72 h,

Table 2. List of the identified histone-associated proteins

Band number	MW (kDa)	Protein	Accession	Category	Reference
1	219.0	Chromodomain helicase DNA binding protein 4 (Mi-2b)	gil39204553	Chromatin remodeling	–
2	181.9	Smarca4 protein (Brg1)	gil50927531	Chromatin remodeling	H4; Agalioti *et al.* 2002
3	207.0	AT rich interactive domain 1A (ARID1A)	gil15808996	Chromatin remodeling	–
	162.0	Cleavage and polyadenylation specific factor 1	gil16751835	Other	–
	152.8	mutS homolog 6 (MSH6)	gil6754744	Other	–
4	123.8	Baf155	gil6678027	Chromatin remodeling	–
	113.5	G7A	gil3986754	Other	–
5	192.0	Nucleoporin 133	gil20071177	Other	–
6	113.5	ADP-ribosyltransferase (NAD+, poly (ADP-ribose) polymerase) 1	gil20806109	Other	H3/H4; Pinnola *et al.* 2007
7	88.2	Heterogenous nuclear ribonucleoprotein U	gil17390825	Other	–
	95.9	LSD1	gil37360004	Histone modification	–
8	76.7	Nucleolin (C23)	gil128843	Histone chaperone	–
9	76.7	Nucleolin (C23)	gil128843	Histone chaperone	–
10	76.7	Nucleolin (C23)	gil128843	Histone chaperone	–
11	64.0	p66α (BC031407 protein)	gil23398610	Chromatin remodeling	H3/H4; Brackertz *et al.* 2006
12	–	NI	–	–	–
13	–	NI	–	–	–
14	55.0	Putative histone deacetylase1 (HDAC1)	gil2347180	Chromatin remodeling	–
	29.2	U1 small nuclear ribonucleoprotein 70 kDa polypeptide A	gil26380180	Other	–
15	58.0	Pendulin (importinα1)	gil1363205	Other	–
	50.9	Heterogenous nuclear ribonucleoprotein K	gil473912	Other	–
16	35.5	Similar to BAF57	gil51782778	Chromatin remodeling	–
	43.4	DEK oncogene	gil29789160	Histone chaperone	–
	50.5	RuvB-like protein 1 (Tip49a)	gil13435708	Other	–
	42.6	β-tubulin	gil202229	Other	–
17	51.8	Chromatin assembly factor 1 subunit C (RbAp48)	gil2494893	Chromatin remodeling	H4; Verreault *et al.* 1998
18	50.1	Elongation factor 1-γ	gil13626388	Other	–
19	50.2	Translation elongation factor eEF-1 α-chain-mouse	gil72870	Other	–
	50.1	Elongation factor 1-γ	gil13626388	Other	–
20	47.4	BRG1/brm-associated factor 53A (Baf53a)	gil9789893	Chromatin remodeling	–
21	38.0	α-actin	gil49864	Other	–
22	41.0	γ-actin	gil809561	Other	–

Table 2. *Continued*

Band number	MW (kDa)	Protein	Accession	Category	Reference
23	22.5	Wdr5 protein	gil14250247	Histone modification	H3; Wysocka *et al.* 2005
	41.0	U5 snRNP-specific protein	gil21313414	Other	–
	34.4	Heterogeneous nuclear ribonucleoprotein C	gil8393544	Other	–
24	30.9	Heterogeneous nuclear ribonucleoprotein A/B	gil6754222	Other	–
25	32.5	Nucleophosmin 1 (NPM1)	gil6679108	Histone chaperone	H3/H4; Okuwaki *et al.* 2001; Swaminathan *et al.* 2005
	39.5	Similar to glyceraldehyde-3-phosphate dehydrogenase	gil28485300	Other	–
26	28.7	Eukaryotic translation elongation factor 1-δ	gil12963597	Other	–
	31.8	Small nuclear ribonucleoprotein polypeptide A	gil13096860	Other	–
27	22.2	Histone 1, H1d	gil34328365	Other	–
28	28.3	Methyl-CpG binding domain protein 3 (MBD3)	gil23398550	Chromatin remodling	–
	21.8	Histone 1, H1a	gil21426823	Other	–
29	24.7	Elongation factor 1-β homolog	gil5902663	Other	–
30	–	NI	–	–	–
31	33.4	SET translocation	gil13591862	Histone chaperone	H3/H4; Kawase *et al.* 1996; Muto *et al.* 2007
	23.9	Small nuclear ribonucleoprotein B	gil6678053	Other	–
32	19.4	Nucleoplasmin 3 (NPM3)	gil6679110	Histone chaperone	–
33	–	NI	–	–	–
34	15.1	Histone H2B	gil280961	Other	H3/H4; Ilyin & Bayev 1975
35	14.0	Small nuclear ribonucleoprotein D3	gil13385598	Other	
36	12.4	Enhancer of rudimentary homolog (ERH)	gil6679685	Other	

The identified proteins are categorized into chromatin remodeling proteins, histone modification related-proteins, histone chaperones, and others. 'NI' represents the proteins that were not identifiable. The numbers in the third right column (Accession) indicate protein database accession numbers. Literatures are cited in 'Reference' that were reported to directly bind to histone H3 and/or H4.

and continued to decrease thereafter. The expression level of NPM3 protein together with that of OCT4 protein in both control and RA-treated cells was estimated by Western blotting on whole cell lysates (Fig. 3B). As expected, ES cells in the undifferentiated state, but not in the differentiated state, showed robust expression of NPM3 and OCT4 protein.

Histone binding activity of NPM3

To characterize binding specificity of NPM3 protein toward the tail domain of core histones, we carried out two types of *in vitro* binding experiments using nuclear extracts of ES cells as a source of the native NPM3 (Fig. 4A, upper panel) and *in vitro* synthesized Flag/NPM3 (Fig. 4A, lower panel). The baits were the tail peptides of histone H3 and H4, and those of histone H2A, H2B, H3, and H4 in the former and the latter binding experiments, respectively. Native NPM3 in the nuclear extracts showed a much higher affinity to the H4 tail peptide than the H3 tail peptide, which supported the previous result (Fig. 1). The *in vitro* synthesized NPM3 also had a high affinity to the H4 tail.

To examine the influence of other domains of histone molecules on the binding of NPM3 to the tail domain, we estimated its binding to whole histone molecules. The histone molecules tested for binding were H2A, H2B, H3, and H4. Flag/NPM3 was incubated with anti-Flag M2 agarose beads and each of the histones. The bead-bound histones were separated by SDS–PAGE (Fig. 4B). No signals of bound histone were observed for histone H2A or H2B. Interestingly, not only histone H4, but also H3 bound to the immobilized NPM3, although the tail domain of H3 alone did not show or showed very little binding activity for the protein (Fig. 4A).

Overexpression of NPM3 gene in ES cells

In order to discover the biological significance of the binding of NPM3 to histone H4 and likely to H3, we investigated the effect of NPM3 overexpression on ES cells. ES cells were transfected with pEGFP-N3/NPM3, together with pEGFP-1 and pEGFP-N3, both as control genes, and were allowed to proliferate for 3 days. Observation via a fluorescence microscopy indicated that the transfection efficiency was about 70%. The expression of the fusion protein, EGFP/NPM3, was verified by Western blot analysis with anti-GFP antisera (Fig. 5A). Overexpression seemed not to affect the pluripotent nature of ES cells, because NPM3-overexpressing ES cells expressed OCT4 (Fig. 5A) and Nanog (data not shown), both pluripotent marker proteins, at levels similar to those observed in control cells. Immunocytochemistry for EGFP/NPM3 showed that NPM3 was distributed in both nucleoli and nuclei (Figs 5B.e and its inset) as reported previously (Huang *et al.* 2005). NPM3 was more concentrated in nucleoli than in nuclei.

NPM1 belongs to the same family as NPM3 and is involved in the regulation of proliferation of mouse ES cells and hematopoietic stem cells (Li *et al.* 2006; Wang *et al.* 2006). Therefore, we compared the proliferation rate among the three types of transfected cells by MTT assay (Fig. 5C). The rate of proliferation of NPM3-overexpressing ES cells was significantly increased by about 1.5-fold over both of the control transfectants ($P < 0.01$). This increase was confirmed by direct cell counting at a level of $P < 0.05$ (data not shown).

Discussion

Nuclear properties and chromatin structures of ES cells have received intensive scrutiny (Meshorer & Misteli 2006; Meshorer *et al.* 2006). Microarray (Kelly & Rizzino 2000; Ramalho-Santos *et al.* 2002) and proteomic analyses are comprehensive and powerful approaches to characterize and further understand self-renewal and pluripotency of ES cells at the gene and protein levels (Guo *et al.* 2001; Kurisaki *et al.* 2005; Nagano *et al.* 2005; Wang & Gao 2005; Baharvand *et al.* 2006; Stanton & Bakre 2007). Our pull-down assay was made on the nuclear proteins of ES cells using synthetic peptides of histone tail domain as baits, because the histone tail domain is considered to play critical roles in the biological functions of histones, not least because histones incorporate target sites for active biochemical modifications that profoundly affect their function. It should be noted that the used baits were synthetic unmodified ('bare') histone tail peptides. The synthetic tails are likely not to receive such modifications, because cofactors necessary for enzymatic modifications of histone such as acetyl-CoA might be lost during preparation. Despite this limitation, we were able to isolate the histone binding proteins that included more than 10 previously reported proteins as histone binding proteins.

Histone H3 and H4 tail peptides showed similar binding profiles toward nuclear proteins. However, the histone H3 tail bait demonstrated a lower binding affinity to most of the proteins relative to the histone H4 tail bait, although the reason for this difference was not elucidated and will require further study. Forty-five proteins were identified as candidates that associate with the histone H4 tail and these were grouped into four broad categories: chromatin

remodeling proteins, histone chaperones, histone modification-related proteins, and others. It is noteworthy that members of the two chromatin remodeling complexes, BAF (Wang *et al.* 1996a, b) and NuRD complex (Zhang *et al.* 1999) were among the most abundant proteins identified. RbAp48 and p66α of them were reported to directly associate with histone H4 (Verreault *et al.* 1998; Brackertz *et al.* 2006). The present study suggests that these chromatin remodeling proteins are significant for differentiation rather than maintenance of pluripotency of ES cells because they were upregulated in the RA-treated ES cells. Five proteins were identified as histone chaperones including NPM3, which is a member of the NPM family (Macarthur & Shackleford 1997; Shackleford *et al.* 2001; Frehlick *et al.* 2007). Histone chaperone directly regulates the chromatin structures (Adkins & Tyler 2004; Tamada *et al.* 2006; Frehlick *et al.* 2007). For example, HIRA, a chaperone of histone H3.3, regulates the binding of histone H3.3 with chromatin in mouse ES cells (Meshorer *et al.* 2006). Histone H3 and H3.3 are thought to be in a dynamic state as to the binding to chromatin in HIRA-knockout ES cells: they are in either an unbound or a more loosely bound state compared with the wild-type cells. This dynamic state of the chromatin structure might be responsible for the observed accelerated differentiation to neurons of the knockout cells. The histone chaperones identified in the present study might be responsible for maintaining the chromatin structures unique to ES cells. It should be noted that NPM3 has not been characterized as a histone H4 tail-binding protein and only this protein was highly expressed in undifferentiated ES cells among the identified proteins in the present study.

Together with NPM1 and NPM2, NPM3 belongs to the NPM family that has important roles in cellular processes such as chromatin remodeling, genome stability, ribosome biogenesis, DNA duplication and transcriptional regulation (Philpott *et al.* 1991; Savkur & Olson 1998; Okuda 2002; Grisendi *et al.* 2005; Huang *et al.* 2005; Tamada *et al.* 2006; Liu *et al.* 2007a, b). NPM1 rapidly increases its expression in response to mitogenic stimuli and is highly expressed in tumor and growing cells (Chan *et al.* 1989; Nozawa *et al.* 1996; Grisendi *et al.* 2006). NPM1 preferentially binds to histone H3 and mediates the nucleosome assembly (Okuwaki *et al.* 2001; Swaminathan *et al.* 2005). NPM2 also binds to histone H2A and H2B, and mediates chromatin assembly of sperms (Dilworth *et al.* 1987; Philpott *et al.* 1991; Tamada *et al.* 2006). The least amount of data are available for NPM3, which is the most recently identified as a NPM3 family member.

Nucleoplasmin 3 was originally identified among the genes activated by mouse tumor virus proviral insertions (Kuriki *et al.* 2000). In human tissues, NPM3 was ubiquitously expressed, preferentially in the pancreas and the testis (Shackleford & Macarthur 2001). It was reported that an antisense oligonucleotide of NPM3 blocks the decondensation of sperm chromatin in fertilized mouse eggs (Mclay & Clarke 2003). Our results demonstrate that NPM3 is capable of binding to the histone H4 tail domain. mRNA and proteins of NPM3 were expressed in the undifferentiated ES cells at higher levels than in the differentiated ES cells. We consider that NPM3 may be a key molecule responsible for maintaining chromatin structures unique to ES cells. NPM3 showed a lower affinity to the H3 tail domain compared with the H4 tail domain under the conditions used in our binding experiments. However, there was no such significant difference in the affinity to NPM3 when tested using the whole histone H3 and H4 molecules. Therefore, it is likely that NPM3 binds to domains of histone H3 other than the tail, or other domains are required for the NPM3 binding to the tail domain.

Nucleoplasmin 3 has been implicated in ribosome biogenesis, which is involved in cell proliferation (Huang *et al.* 2005). Thus, it is plausible that NPM3 stimulates proliferation of ES cells through regulating chromatin structure of the rRNA gene. This possibility appears to be consistent with the nucleolar distribution of NPM3 as suggested by Huang *et al.* (2005). There is still another possibility about the mechanism of stimulation of ES cells by NPM3. NPM1 stimulates the proliferation of mouse ES cells (Wang *et al.* 2006). In addition, it has been reported that NPM3 directly interacts with NPM1 (Huang *et al.* 2005). Our preliminary experiments also showed that NPM3 forms a complex with NPM1 in mouse ES cell lysates (data not shown). Therefore, it is most likely that NPM3 regulates the ES cell proliferation through interaction with NPM1 and possibly with other cell cycle regulators.

As a preliminary study, we made NPM3 gene knock-down experiments with mouse ES cells under conditions that had been commonly used in the gene knock-down study with ES cells. However, these trials were unsuccessful. Instead, we successfully knocked-down NPM3 genes in P19 cells, a mouse embryonal carcinoma cell line. These downregulated cells showed no alterations of phenotypes as to proliferation and expressions of Nanog and OCT4 genes. Thus, it is strongly suggested that other protein(s) will compensate NPM3 as its role in proliferation of ES cells if NPM3 gene knock-down ES cells would be successfully generated.

Acknowledgements

This study was supported by a grant from Hiroshima University 21st Century COE Program for Advanced Radiation Casualty Medicine, Hiroshima University, Japan. A part of this study was carried out in collaboration with and with financial support from Intercytex and Prophoenix.

References

Adkins, M. & Tyler, J. 2004. The histone chaperone Asf1p mediates global chromatin disassembly *in vivo*. *J. Biol. Chem.* **279**, 52 069–52 074.

Agalioti, T., Chen, G. & Thanos, D. 2002. Deciphering the transcriptional histone acetylation code for a human gene. *Cell* **111**, 381–392.

Baharvand, H., Hajheidari, M., Ashtiani, S. & Salekdeh, G. 2006. Proteomic signature of human embryonic stem cells. *Proteomics* **6**, 3544–3549.

Brackertz, M., Gong, Z., Leers, J. & Renkawitz, R. 2006. p66alpha and p66beta of the Mi-2/NuRD complex mediate MBD2 and histone interaction. *Nucl. Acids Res.* **34**, 397–406.

Carlson, M. & Laurent, B. 1994. The SNF/SWI family of global transcriptional activators. *Curr. Opin. Cell Biol.* **6**, 396–402.

Chambers, I., Colby, D., Robertson, M. *et al.* 2003. Functional expression cloning of Nanog, a pluripotency sustaining factor in embryonic stem cells. *Cell* **113**, 643–655.

Chan, W., Liu, Q., Borjigin, J. *et al.* 1989. Characterization of the cDNA encoding human nucleophosmin and studies of its role in normal and abnormal growth. *Biochemistry* **28**, 1033–1039.

Dilworth, S., Black, S. & Laskey, R. 1987. Two complexes that contain histones are required for nucleosome assembly *in vitro*: role of nucleoplasmin and N1 in Xenopus egg extracts. *Cell* **51**, 1009–1018.

Eirín-López, J., Frehlick, L. & Ausió, J. 2006. Long-term evolution and functional diversification in the members of the nucleophosmin/nucleoplasmin family of nuclear chaperones. *Genetics* **173**, 1835–1850.

Evans, M. & Kaufman, M. 1981. Establishment in culture of pluripotential cells from mouse embryos. *Nature* **292**, 154–156.

Frehlick, L., Eirín-López, J. & Ausió, J. 2007. New insights into the nucleophosmin/nucleoplasmin family of nuclear chaperones. *Bioessays* **29**, 49–59.

Grisendi, S., Bernardi, R., Rossi, M. *et al.* 2005. Role of nucleophosmin in embryonic development and tumorigenesis. *Nature* **437**, 147–153.

Grisendi, S., Mecucci, C., Falini, B. & Pandolfi, P. 2006. Nucleophosmin and cancer. *Nat. Rev. Cancer* **6**, 493–505.

Guo, X., Ying, W., Wan, J. *et al.* 2001. Proteomic characterization of early-stage differentiation of mouse embryonic stem cells into neural cells induced by all-trans retinoic acid in vitro. *Electrophoresis* **22**, 3067–3075.

Hsu, D., Economides, A., Wang, X., Eimon, P. & Harland, R. 1998. The Xenopus dorsalizing factor Gremlin identifies a novel family of secreted proteins that antagonize BMP activities. *Mol. Cell* **1**, 673–683.

Huang, N., Negi, S., Szebeni, A. & Olson, M. 2005. Protein NPM3 interacts with the multifunctional nucleolar protein B23/nucleophosmin and inhibits ribosome biogenesis. *J. Biol. Chem.* **280**, 5496–5502.

Ilyin, Y. & Bayev, A. J. 1975. Histone–histone interactions as revealed by formaldehyde treatment of chromatin. *Mol. Biol. Rep.* **2**, 159–165.

Jenuwein, T. & Allis, C. 2001. Translating the histone code. *Science* **293**, 1074–1080.

Kawase, H., Okuwaki, M., Miyaji, M. *et al.* 1996. NAP-I is a functional homologue of TAF-I that is required for replication and transcription of the adenovirus genome in a chromatin-like structure. *Genes Cells* **1**, 1045–1056.

Kelly, D. & Rizzino, A. 2000. DNA microarray analyses of genes regulated during the differentiation of embryonic stem cells. *Mol. Reprod. Dev.* **56**, 113–123.

Kuriki, K., Kamiakito, T., Yoshida, H., Saito, K., Fukayama, M. & Tanaka, A. 2000. Integration of proviral sequences, but not at the common integration sites of the FGF8 locus, in an androgen-dependent mouse mammary Shionogi carcinoma. *Cell Mol. Biol. (Noisy-le-Grand)* **46**, 1147–1156.

Kurisaki, A., Hamazaki, T., Okabayashi, K. *et al.* 2005. Chromatin-related proteins in pluripotent mouse embryonic stem cells are downregulated after removal of leukemia inhibitory factor. *Biochem. Biophys. Res. Commun.* **335**, 667–675.

Lee, L., Mortensen, R., Larson, C. & Brent, G. 1994. Thyroid hormone receptor-alpha inhibits retinoic acid-responsive gene expression and modulates retinoic acid-stimulated neural differentiation in mouse embryonic stem cells. *Mol. Endocrinol.* **8**, 746–756.

Li, J., Sejas, D., Rani, R., Koretsky, T., Bagby, G. & Pang, Q. 2006. Nucleophosmin regulates cell cycle progression and stress response in hematopoietic stem/progenitor cells. *J. Biol. Chem.* **281**, 16 536–16 545.

Liu, H., Tan, B., Tseng, K. *et al.* 2007a. Nucleophosmin acts as a novel AP2alpha-binding transcriptional corepressor during cell differentiation. *EMBO Rep.* **8**, 394–400.

Liu, X., Liu, Z., Jang, S. *et al.* 2007b. Sumoylation of nucleophosmin/B23 regulates its subcellular localization, mediating cell proliferation and survival. *Proc. Natl Acad. Sci. USA*, **104**, 9679–9684.

Macarthur, C. & Shackleford, G. 1997. Npm3: a novel, widely expressed gene encoding a protein related to the molecular chaperones nucleoplasmin and nucleophosmin. *Genomics* **42**, 137–140.

Masui, S., Nakatake, Y., Toyooka, Y. *et al.* 2007. Pluripotency governed by Sox2 via regulation of Oct3/4 expression in mouse embryonic stem cells. *Nat. Cell Biol.* **9**, 625–635.

Matsuda, T., Nakamura, T., Nakao, K. *et al.* 1999. STAT3 activation is sufficient to maintain an undifferentiated state of mouse embryonic stem cells. *EMBO J.* **18**, 4261–4269.

McLay, D. & Clarke, H. 2003. Remodelling the paternal chromatin at fertilization in mammals. *Reproduction* **125**, 625–633.

Meshorer, E. & Misteli, T. 2006. Chromatin in pluripotent embryonic stem cells and differentiation. *Nat. Rev. Mol. Cell Biol.* **7**, 540–546.

Meshorer, E., Yellajoshula, D., George, E., Scambler, P., Brown, D. & Misteli, T. 2006. Hyperdynamic plasticity of chromatin proteins in pluripotent embryonic stem cells. *Dev. Cell* **10**, 105–116.

Misteli, T. 2001. Protein dynamics: implications for nuclear architecture and gene expression. *Science* **291**, 843–847.

Mitsui, K., Tokuzawa, Y., Itoh, H. *et al.* 2003. The homeoprotein Nanog is required for maintenance of pluripotency in mouse epiblast and ES cells. *Cell* **113**, 631–642.

Muto, S., Senda, M., Akai, Y. *et al.* 2007. Relationship between the structure of SET/TAF-Ibeta/INHAT and its histone

chaperone activity. *Proc. Natl Acad. Sci. USA* **104**, 4285–4290.

Nagano, K., Taoka, M., Yamauchi, Y. *et al.* 2005. Large-scale identification of proteins expressed in mouse embryonic stem cells. *Proteomics* **5**, 1346–1361.

Nichols, J., Zevnik, B., Anastassiadis, K. *et al.* 1998. Formation of pluripotent stem cells in the mammalian embryo depends on the POU transcription factor Oct4. *Cell* **95**, 379–391.

Nozawa, Y., Van Belzen, N., Van Der Made, A., Dinjens, W. & Bosman, F. 1996. Expression of nucleophosmin/B23 in normal and neoplastic colorectal mucosa. *J. Pathol* **178**, 48–52.

Ogawa, K., Matsui, H., Ohtsuka, S. & Niwa, H. 2004. A novel mechanism for regulating clonal propagation of mouse ES cells. *Genes Cells* **9**, 471–477.

Okuda, M. 2002. The role of nucleophosmin in centrosome duplication. *Oncogene* **21**, 6170–6174.

Okuwaki, M., Matsumoto, K., Tsujimoto, M. & Nagata, K. 2001. Function of nucleophosmin/B23, a nucleolar acidic protein, as a histone chaperone. *FEBS Lett.* **506**, 272–276.

Philpott, A., Leno, G. & Laskey, R. 1991. Sperm decondensation in Xenopus egg cytoplasm is mediated by nucleoplasmin. *Cell* **65**, 569–578.

Pinnola, A., Naumova, N., Shah, M. & Tulin, A. 2007. Nucleosomal core histones mediate dynamic regulation of poly (ADP-ribose) polymerase 1 protein binding to chromatin and induction of its enzymatic activity. *J. Biol. Chem.* **282**, 32 511–32 519.

Ramalho-Santos, M., Yoon, S., Matsuzaki, Y., Mulligan, R. & Melton, D. 2002. 'Stemness': transcriptional profiling of embryonic and adult stem cells. *Science* **298**, 597–600.

Savkur, R. & Olson, M. 1998. Preferential cleavage in pre-ribosomal RNA byprotein B23 endoribonuclease. *Nucl. Acids Res.* **26**, 4508–4515.

Shackleford, G., Ganguly, A. & MaCarthur, C. 2001. Cloning, expression and nuclear localization of human NPM3, a member of the nucleophosmin/nucleoplasmin family of nuclear chaperones. *BMC Genomics* **2**, 8.

Stanton, L. & Bakre, M. 2007. Genomic and proteomic characterization of embryonic stem cells. *Curr. Opin. Chem. Biol.* **11**, 399–404.

Swaminathan, V., Kishore, A., Febitha, K. & Kundu, T. 2005. Human histone chaperone nucleophosmin enhances acetylation-dependent chromatin transcription. *Mol. Cell Biol.* **25**, 7534–7545.

Takahashi, K., Tanabe, K., Ohnuki, M. *et al.* 2007. Induction of pluripotent stem cells from adult human fibroblasts by defined factors. *Cell* **131**, 861–872.

Takahashi, K. & Yamanaka, S. 2006. Induction of pluripotent stem cells from mouse embryonic and adult fibroblast cultures by defined factors. *Cell* **126**, 663–676.

Tamada, H., Van Thuan, N., Reed, P. *et al.* 2006. Chromatin decondensation and nuclear reprogramming by nucleoplasmin. *Mol. Cell Biol.* **26**, 1259–1271.

Turner, B. 2002. Cellular memory and the histone code. *Cell* **111**, 285–291.

Tuteja, R. & Tuteja, N. 1998. Nucleolin: a multifunctional major nucleolar phosphoprotein. *Crit. Rev. Biochem. Mol. Biol.* **33**, 407–436.

Verreault, A., Kaufman, P., Kobayashi, R. & Stillman, B. 1998. Nucleosomal DNA regulates the core-histone-binding subunit of the human Hat1 acetyltransferase. *Curr. Biol.* **8**, 96–108.

Wang, W., Côté, J., Xue, Y. *et al.* 1996a. Purification and biochemical heterogeneity of the mammalian SWI-SNF complex. *EMBO J.* **15**, 5370–5382.

Wang, D. & Gao, L. 2005. Proteomic analysis of neural differentiation of mouse embryonic stem cells. *Proteomics* **5**, 4414–4426.

Wang, B., Lu, R., Wang, W. & Jin, Y. 2006. Inducible and reversible suppression of Npm1 gene expression using stably integrated small interfering RNA vector in mouse embryonic stem cells. *Biochem. Biophys. Res. Commun.* **347**, 1129–1137.

Wang, W., Xue, Y., Zhou, S., Kuo, A., Cairns, B. & Crabtree, G. 1996b. Diversity and specialization of mammalian SWI/SNF complexes. *Genes Dev* **10**, 2117–2130.

Williams, R., Hilton, D., Pease, S. *et al.* 1988. Myeloid leukaemia inhibitory factor maintains the developmental potential of embryonic stem cells. *Nature* **336**, 684–687.

Wysocka, J., Swigut, T., Milne, T. *et al.* 2005. WDR5 associates with histone H3 methylated at K4 and is essential for H3, K4 methylation and vertebrate development. *Cell* **121**, 859–872.

Yamagata, A., Kristensen, D., Takeda, Y. *et al.* 2002. Mapping of phosphorylated proteins on two-dimensional polyacrylamide gels using protein phosphatase. *Proteomics* **2**, 1267–1276.

Zhang, Y., Ng, H., Erdjument-Bromage, H., Tempst, P., Bird, A. & Reinberg, D. 1999. Analysis of the NuRD subunits reveals a histone deacetylase core complex and a connection with DNA methylation. *Genes Dev* **13**, 1924–1935.

Successful *in vivo* propagation of factor IX-producing hepatocytes in mice: Potential for cell-based therapy in haemophilia B

Kohei Tatsumi[1], Kazuo Ohashi[2, 5], Miho Kataoka[3], Chise Tateno[3, #], Masaru Shibata[1], Hiroyuki Naka[1], Midori Shima[1], Michiyoshi Hisanaga[2], Hiromichi Kanehiro[2], Teruo Okano[5], Katsutoshi Yoshizato[3, 4, #], Yoshiyuki Nakajima[2], Akira Yoshioka[1]

[1]Department of Pediatrics, Nara Medical University, Nara, Japan; [2]Department of Surgery, Nara Medical University, Nara, Japan; [3]Yoshizato Project, Cooperative Link of Unique Science and Technology for Economy Revitalization (CLUSTER), Hiroshima Prefectural Institute of Industrial Science and Technology, Hiroshima, Japan; [4]Graduate School of Science, Hiroshima University, Hiroshima, Japan; [5]Institute of Advanced Biomedical Engineering and Science, Tokyo Women's Medical University, Tokyo, Japan

Summary

Cell-based therapies using isolated hepatocytes have been proposed to be an attractive application in the treatment of haemophilia B due to the normal production of coagulation factor IX (FIX) in these particular cells. Current cell culture technologies have largely failed to provide adequate isolated hepatocytes, so the present studies were designed to examine a new approach to efficiently proliferate hepatocytes that can retain normal biological function, including the ability to synthesize coagulation factors like FIX. Canine or human primary hepatocytes were transplanted into urokinase-type plasminogen activator-severe combined immunodeficiency (uPA/SCID) transgenic mice. Both donor hepatocytes from canines and humans were found to progressively proliferate in the recipient mouse livers as evidenced by a sharp increase in the circulating blood levels of species-specific albumin, which was correlated with the production and release of canine and human FIX antigen levels into the plasma. Histological examination confirmed that the transplanted canine and human hepatocytes were able to proliferate and occupy >80% of the host livers. In addition, the transplanted hepatocytes demonstrated strong cytoplasmic staining for human FIX, and the secreted coagulation factor IX was found to be haemostatically competent using specific procoagulant assays. In all, the results from the present study indicated that developments based on this technology could provide sufficient FIX-producing hepatocytes for cell-based therapy for haemophilia B.

Keywords

Haemophilia A/B, haemophilia therapy, coagulation factors, hepatology

Thromb Haemost 2008; 99: 883–891

Introduction

Haemophilia B is a rare X-chromosome-linked recessive bleeding disorder, caused by a failure in the production of functional coagulation factor IX (FIX), and this disease affects ~1 in 30,000 males (1, 2). The main clinical manifestation of this disease is similar to haemophilia A (factor VIII deficiency), and under severe conditions the affected patient can be found to have unpredictable, recurrent, spontaneous bleeding in various areas, including soft tissues, major joints and occasionally in internal organs. In these circumstances, the onset and progression of chronic haemoarthropathy leads to a marked disruption in the physical and social aspects of the affected patients. Standard treatment for haemophilia B is either on-demand or prophylactic therapy with plasma-derived or recombinant human FIX concentrates. This type of treatment requires frequent intravenous infusion, which can be a potential biohazard from blood-borne viral infections to the patient if the infusate is derived from a heterogeneous population of human blood. In addition, the high cost of commercial concentrates and the life-long requirement for replacement therapy can have a significant impact on economic resources. In an attempt to resolve these difficulties, longer acting

Correspondence to:
Kazuo Ohashi, MD, PhD
Institute of Advanced Biomedical Engineering and Science
Tokyo Women's Medical University
8–1 Kawada-cho, Shinjuku-ku, Tokyo, 162–8666, Japan
Tel.: +81 3 3353 8111, ext 66214, Fax: +81 3 3359 6046
E-mail: ohashi@abmes.twmu.ac.jp

Present address: PhoenixBio Co. Ltd, Hiroshima, Japan.

Financial support:
This study was supported in part by The Leading Projects (K.O. and T.O.) and Grant-in-Aid (no. 18591957 to K.O.) from the Scientific Research from the Ministry of Education, Science, Sport and Culture of Japan, grants for AIDS Research from the Ministry of Health, Labor and Welfare of Japan (A.Y.), and grant for CLUSTER (K.Y.).

Received September 12, 2007
Accepted after major revision March 12, 2008

Prepublished online April 9, 2008
doi:10.1160/TH07-09-0559

and safer therapeutic strategies have been investigated. For example, gene therapy using viral vectors has been extensively studied in the past decade (3), and although therapeutic and long-term efficacy has been demonstrated in animal models (4–12), clinical trials have not conclusively shown long-term therapeutic benefit (13, 14). It seems likely, therefore, that alternate therapeutic options will need to be developed.

Recent clinical success with liver transplantation in haemophilia has encouraged further investigation into cell-based therapies (15–17). In haemophilia B patients, elevations in biologically active FIX levels from <1.0% to >1.0%, can alter the phenotype from severe to moderate resulting in a marked improvement in the symptomology and quality of life (1). Coagulation FIX is synthesized in hepatocytes (18), and so cell-based therapies using isolated hepatocytes could provide therapeutic potential. Hepatocytes also produce other coagulation factors, such as factors VII and VIII (19–24), and it may be that this type of treatment could have broader applications to not only haemophlia B, but other coagulation deficiencies. Recently, we have adopted several approaches to bioengineer functional liver tissue *in vivo* (25–30). We have demonstrated that isolated hepatocytes transplanted under the kidney capsule in haemophilia A mice produced therapeutic plasma FVIII activity and corrected the phenotypic defect (28). Dhawan et al. (31) also recently described the therapeutic benefits of hepatocyte transplantation in congenital factor VII deficiency, and the relative technical simplicity of cell-based therapy may offer a significant and technological advantage.

One of the major hurdles in establishing this type of therapy is the limited availability of biologically functional hepatocytes. At present, the number of donor livers remains severely restricted and even if they are available, these livers are frequently of marginal quality (32). Current procedures for the culture of primary hepatocytes do not appear to support extensive cell proliferation (33), so methods to circumvent this problem have recently been studied, but their role to treat haemophilia were not examined. Isolated hepatocytes were genetically modified via transfection with an immortalizing gene, such as simian virus 40 large T antigen, to promote long-term survival (34), but FIX gene expression and production was not investigated. Although the genetic manipulation of hepatocytes can be achieved following isolation *in vitro*, this type of approach to promote hepatocyte proliferation is not a trivial matter *in vivo*. Towards this end, methods to provide proliferative stimuli has been studied *in vivo*, such as a reduction in existing liver mass, or alternatively in a condition where there is likely to be a selective advantage for transplanted cells to proliferate (26, 28). Due to these limitations, we investigated a different method to isolate and proliferate hepatocytes that can retain the hepatic machinery to sustain the synthesis of coagulation factors, such as FIX. In the present study, we studied whether transplantation of canine or human primary hepatocytes into urokinase-type plasminogen activator-severe combined immunodeficiency (uPA/SCID) transgenic mice could enhance the production of coagulation factor IX. The uPA/SCID mouse has been previously shown to have hepatic parenchymal cell damage, which results in the continuous release of regenerative stimuli (35), so we believed that the hepatic environment may be more conducive to the engraftment of *in vitro* isolated hepatocytes. The functionality of the transplanted hepatocytes was assessed in terms of FIX mRNA and protein production and biological activity as a means to treat haemophilia B.

Materials and methods

Animals

Normal beagles were purchased from Oriental BioService, Inc. (Kyoto, Japan). C57BL/6 mice were purchased from Jackson Laboratory (Bar Harbor, ME, USA). uPA/SCID mice were generated at Hiroshima Prefectural Institute of Industrial Science and Technology (Higashihiroshima, Hiroshima, Japan) as described previously (35). Genotyping for the presence of the uPA transgene in the SCID mice was confirmed by polymerase chain reaction (PCR) assay of isolated genomic DNA as described previously (35, 36). Experimental protocols were developed in accordance with the guidelines of the local animal committees located at both Hiroshima Prefectural Institute of Industrial Science and Technology and Nara Medical University.

Hepatocyte isolation

Canine hepatocytes were isolated from livers (~100 g piece) harvested from two normal beagles (Dog 1: 7-year-old male and Dog 2: 1-year-old female) by a two-step perfusion method using 0.05% collagenase (Collagenase S1, Nitta Gelatin, Osaka, Japan) as described previously (25, 27). Cells were then filtered and hepatocytes were separated from non-parenchymal cells by sequential low speed centrifugation at 50 x g followed by Percoll (Percoll™, Amersham Biosciences, Uppsala, Sweden) isodensity centrifugation. The viabilities of the isolated canine hepatocytes were 96.5% and 98.0% as determined by the trypan blue exclusion test. Hepatocytes were kept at 4°C until transplantation. Human hepatocytes, isolated from a one-year-old white male and a six-year-old Afro-American female, were purchased from In Vitro Technologies (Baltimore, MD, USA). The cryopreserved hepatocytes were thawed and suspended in transplant medium (35, 37). The viabilities of thawed human hepatocytes were determined to be 64.4% and 49.2%, respectively.

Transplantation of hepatocytes for the creation of canine- or human-chimeric mice

One day prior to transplantation and one week after transplantation, the uPA/SCID mice, 20 to 30 days old, received intraperitoneal injections of 0.1 mg of anti-asialo GM1 rabbit serum (Wako Pure Chemical Industries Ltd., Osaka, Japan) to inhibit recipient natural killer cell activity against the transplanted hepatocytes. Viable canine- (1.0×10^6) or human- (0.75×10^6) hepatocytes were transplanted using an infusion technique into the inferior splenic pole in which the transplanted cells flow from the spleen into the liver via the portal system. After transplantation, the uPA/SCID mice were treated with nafamostat mesilate to inhibit complement factors activated by canine or human hepatocytes as previously described (35).

Measurement of plasma levels of albumin, FIX antigen and FIX activity

Periodically, retroorbital bleeding was performed in recipient mice, and the blood was collected in a tube containing 0.1 vol

3.8% sodium citrate. Plasma samples were stored at –80°C until analyzed. To assess the proliferating status of transplanted canine hepatocytes, we determined the plasma levels of canine albumin in the recipient plasma by ELISA using primary goat anti-dog albumin and secondary HRP-conjugated goat anti-dog albumin antibodies (Bethyl Laboratories Inc., Montgomery, TX, USA), respectively. For the assessment of proliferation in transplanted human hepatocytes, we similarly measured the blood levels of human albumin by ELISA (Human Albumin ELISA Quantitation kit, Bethyl Laboratories Inc.). The proportion of proliferating donor hepatocytes in the recipient liver (repopulation rate) was determined based on blood albumin levels (35, 38). Human and canine FIX antigen (FIX:Ag) were measured in recipient plasma by ELISA (Asserachrom IX:Ag, Diagnostica Stago, Asnières, France). Human FIX:Ag levels were measured according to the instructions provided by the manufacturer, and canine FIX:Ag levels were quantified by elongating the enzymatic color reaction step. No cross-reactivity with pooled mouse plasma was observed in this ELISA. FIX activity (FIX:C) was measured by one-stage clotting assay based on the activated partial thromboplastin time using human FIX-deficient plasma (bioMerieux Inc., Durham, NC, USA). Pooled canine plasma collected from 75 normal dogs, and normal human plasma (Verify 1, bioMerieux Inc.) were used as reference standards.

Immunohistochemistry for albumin and FIX

Formalin-fixed, paraffin-embedded liver sections from mice transplanted with canine hepatocytes were sectioned and incubated with a primary goat antibody against canine albumin (Bethyl Laboratories Inc.) at a dilution of 1:1,000. The bound antibody was detected by the avidin-biotin complex immunoperoxidase technique using an ABC Elite kit (Vector Laboratories, Burlingame, CA, USA) followed by developing with DAB (3, 3'-diaminobenzine tetrahydrochloride). Expression of human FIX in recipient mice was determined by immunofluorescent staining of frozen liver sections embedded in O.C.T compound

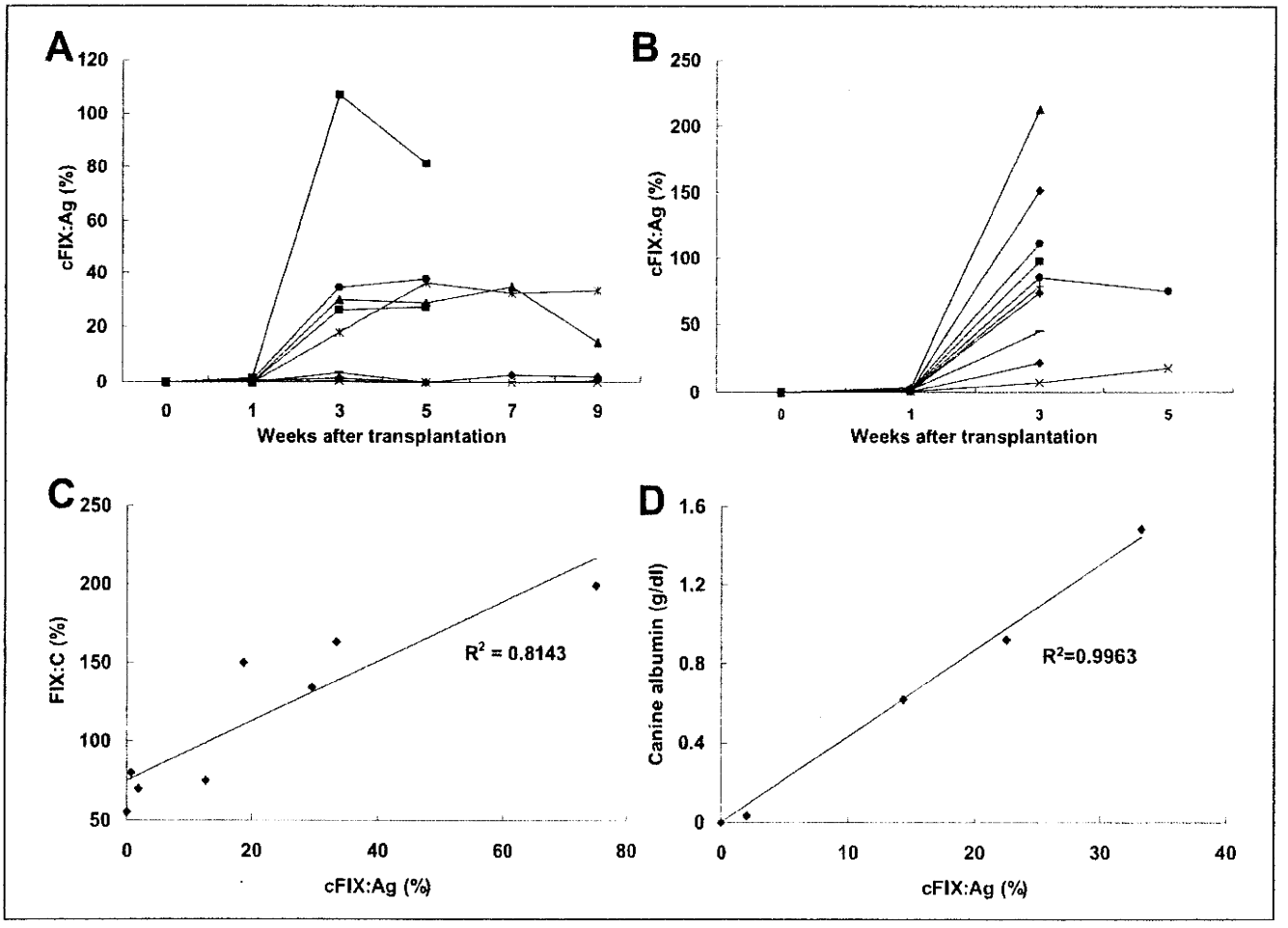

Figure 1: Proliferation of transplanted canine hepatocytes in uPA/SCID mouse livers assessed by recipient plasma analyses. A, B) Plasma canine factor IX (FIX) antigen (cFIX:Ag) levels in uPA/SCID mice after transplantation of hepatocytes isolated from a seven-year-old dog (A) and a one-year-old dog (B) (n=8, 10 in A and B, respectively) (% of pooled normal canine plasma). C) Relationship between total plasma FIX coagulation activity (FIX:C; reflecting both murine and canine FIX activities) (% of normal human plasma) and plasma cFIX:Ag levels of uPA/SCID mice transplanted with canine hepatocytes. D) Relationship between plasma canine albumin concentrations and plasma cFIX:Ag levels of uPA/SCID mice transplanted with canine hepatocytes.

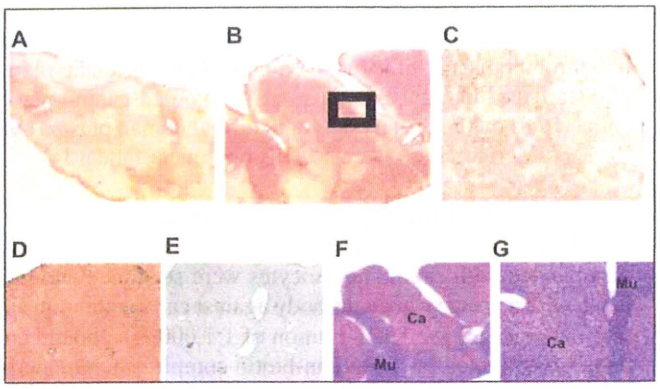

Figure 2: Mouse liver chimerism with proliferated canine hepatocytes. A-E) Immunohistochemical staining of canine albumin in liver sections of uPA/SCID mice transplanted with canine hepatocytes. Representative photomicrographs from a recipient mouse with low plasma cFIX:Ag (2.0% of normal canine plasma) (A) and a mouse with high plasma cFIX:Ag (33.2% of normal canine plasma) (B). C) Higher magnification view of the area outlined in (B). Canine albumin staining of positive control (normal dog liver) (D) and negative control (non-transplanted uPA/SCID mouse liver) (E) indicate the antibody used is specific for canine albumin. F, G) Hematoxylin and Eosin staining on the serial sections of mouse liver from (B). Ca, transplanted canine hepatocytes; Mu, recipient murine liver tissue. Original magnifications, ×40 (A, B, F), ×100 (D,E), and ×200 (C, G).

(Sakura Finetek, Torrance, CA, USA). The sections were incubated overnight at 4°C with the goat anti-human FIX antibody (Affinity Biologicals, Hamilton, ON, Canada) followed by Alexa Fluor 555 rabbit anti-goat IgG (Molecular Probes, Carlsbad, CA, USA) for 60 minutes. Stained sections were subsequently imaged using an Olympus BX51 microscope (Tokyo, Japan) and photographed using an Olympus DP70 digital camera with DP controller and DP manager computer software.

Quantitative real-time PCR

Total RNA was extracted from the liver of all recipient mice, and normal human and canine liver samples using the RNeasy Mini Kit (Qiagen, Hilden, Germany). Normal human liver tissue portions were obtained from surgical specimens at liver surgery for metastatic liver tumours after acquiring written informed consent for the experimental use of harvested liver samples. Extracted RNA (1 µg) was reverse transcribed using oligo $d(T)_{16}$ primers and Omniscript RT Kit (Qiagen). First-strand cDNA samples were subsequently subjected to PCR amplification using the PRISM 7700 Sequence Detector (Applied Biosystems Japan Ltd., Tokyo, Japan). Canine glyceraldehydes-3-phosphate dehydrogenase (GAPDH) and canine FIX sequences were detected using the following primers. The PCR primers for canine GAPDH sequence were forward, 5'CCCCACCCCCAATGTATCA3', reverse, 5'GTCGTCATATTTGGCAGCTTTCT3', and probe, 5'TGTGGATCTGACCTGCCGCCTG3'.
The primers for canine FIX sequence were forward, 5'GTTGTTGGTGGAAAAGATGCC3', reverse, 5'TGCATCAACTTTCCCATTCAAA3', probe, 'CCAGGTCAATTCCCTTGGCAGGTCC3'. TaqMan probes and primers for human sequences were Hs99999905_m1 (GAPDH) and Hs00609168_m1 (FIX) (TaqMan Gene Expression Assay, Applied Biosystems). The relative RNA copy numbers of canine FIX and human FIX in each transplanted mouse were calculated in terms of canine FIX / canine GAPDH or human FIX / human GAPDH expression ratio, respectively. RNA expression of murine FIX and murine GAPDH, combined with cDNA synthesis and real-time PCR using TaqMan probes, Mm99999915_g1 (murine GAPDH) and Mm01308427_m1 (murine FIX) (Applied Biosystems), were similarly assessed in hepatectomy experiments (see below).

Hepatectomy experiment

For the purpose of investigating the FIX mRNA expression during liver regeneration, liver proliferation stimuli was induced by performing a 70% partial hepatectomy on C57BL6 wild-type mice (n=6) as described previously (39). The resected liver lobes were used as our control for a liver sample under quiescence while the remnant liver lobes removed two days after hepatectomy were used as our proliferating samples. Mouse FIX mRNA and mouse GAPDH mRNA expression was assessed on both quiescent and proliferating liver samples as described above.

Statistical analysis

Significant differences were tested by the Wilcoxon t-test between paired groups and by the Mann-Whitney U-test between unpaired groups. Differences between three or more groups were tested by the Kruskal Wallis H-test. If the probability (p) value was less than 0.05, the Mann-Whitney U-test with Bonferroni correction was used to compare each individual group with the appropriate control. All statistical analyses were performed using Excel (Microsoft) with ystat2006 software (Igakutosyo-syuppan, Tokyo, Japan). $P<0.05$ was considered significant.

Results

Proliferation of FIX-producing canine hepatocytes in uPA/SCID mouse livers

Canine hepatocytes isolated from a seven-year-old and a one-year-old beagle were transplanted into uPA/SCID mice (n=8 and 10, respectively). Canine FIX:Ag was detected in the plasma of five out of eight mice three weeks after transplantation with the isolated hepatocytes from the seven-year-old beagle. In four out of the five mice, the FIX:Ag levels reached between 20–40% of normal canine plasma levels for FIX:Ag (Fig. 1A). One transplanted mouse was detected to have nearly 100% of normal canine plasma FIX:Ag levels. In general, the uPA/SCID mice that received hepatocytes from the one-year-old beagle demonstrated a greater rise in the circulating canine FIX:Ag, and 70% of the mice (7 out of 10) showed levels greater than 50% of normal levels three weeks after transplantation (median: 81.8%; Fig. 1B).

Plasma FIX:C was measured using a one-stage clotting assay. The FIX:C of normal canine pooled plasma and untreated uPA/SCID mouse plasma (n=4) was approximately 200% and 50% of normal human plasma, respectively. The FIX:C in the recipient uPA/SCID mice with high canine FIX:Ag levels was greater than in untreated mice or recipient uPA/SCID mice with low FIX:Ag levels (R^2=0.8143) (Fig. 1C). These observations confirmed that the secreted FIX protein had functional coagulation activity.

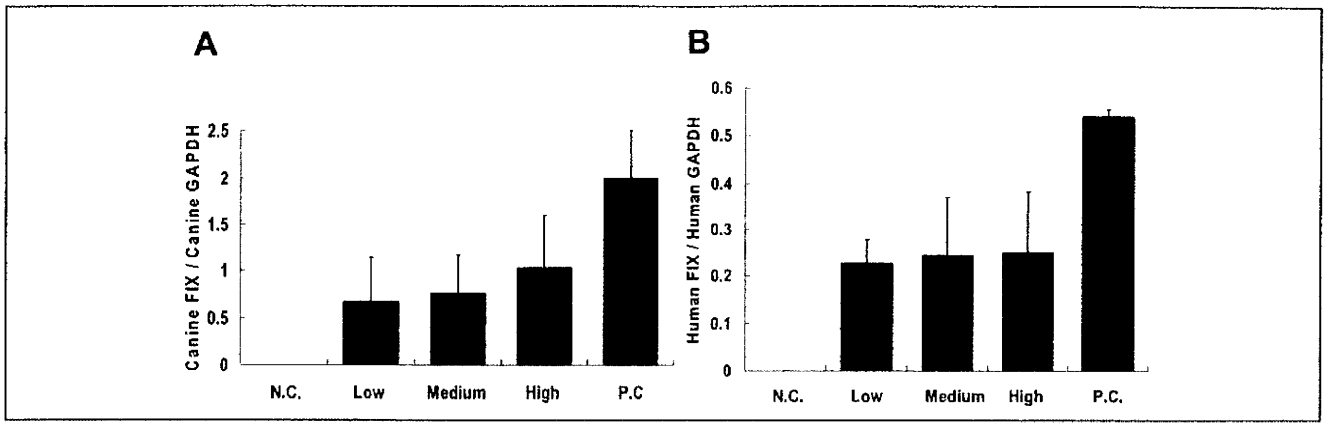

Figure 3: Donor species-specific FIX mRNA expressions in uPA/SCID mouse livers transplanted with either canine or human hepatocytes. A) Canine factor IX (FIX) RNA copy numbers relative to canine GAPDH (reflecting RNA copy numbers per canine hepatocyte), based on plasma cFIX:Ag levels. (Low, <40%; Medium, 41–80%; High, >81% of normal canine plasma. n=4, 4, and 5, respectively). N.C.; negative control: non-transplanted uPA/SCID mouse livers (n=4), P.C.; positive control: normal beagle dog livers (n=3). B) Human FIX RNA copy numbers relative to human GAPDH (reflecting RNA copy numbers per human hepatocyte), based on the repopulation rate (R.R.) estimated from human albumin concentrations as described in *Materials and methods*. (Low, <40%; Medium, 41–65%; High, >66%. n=4, 4, and 4 respectively). N.C., negative control: non-transplanted uPA/SCID mouse livers (n=4); P.C., positive control: normal human liver tissues (n=3).

We also measured canine albumin levels in the plasma of several uPA/SCID mice that received hepatocytes from the seven-year-old beagle, and demonstrated a highly significant correlation between the canine albumin and canine FIX:Ag levels (R^2=0.9963) (Fig. 1D). Assuming that the plasma concentrations of albumin and FIX:Ag in normal dogs are 5 g/dl and 5,000 ng/ml, respectively, the weight ratio of albumin to FIX:Ag in normal canine plasma was calculated to be 10,000:1. These data suggested that the synthesis of canine FIX and albumin in the transplanted animals was similar to that of normal canine liver (i.e. 15% FIX:Ag of normal canine plasma corresponds to 750 ng/ml, and the ratio of 0.6 g/dl to 750 ng/ml approximates to 10,000:1). Immunohistochemical staining for canine albumin in sections obtained at day 55 after transplantation demonstrated a large area of the liver was positive in the recipients with high plasma canine FIX:Ag (33.2%) (Fig. 2B-C), whereas only a small area of liver was positive in mice with low plasma FIX:Ag levels (2.0%) (Fig. 2A). Histological examination of serial liver sections revealed that the canine albumin-positive area was composed of morphologically normal hepatocytes (Fig. 2D-E) indicating that the normal canine hepatocytes had progressively propagated in the uPA/SCID livers.

The uPA/SCID mice that received canine hepatocytes were divided into three groups according to their plasma canine FIX:Ag levels (low <40%, medium 41–80%, and high >81%). mRNA levels of canine FIX were normalized using canine GAPDH mRNA measurements (FIX / GAPDH). As shown in Figure 3A, canine FIX / canine GAPDH expression was similar in the three groups with no statistically significant difference. This suggests that canine hepatocytes proliferated within the uPA/SCID livers without reducing the steady-state levels of canine FIX gene expression and/or degradation. We confirmed that RNA samples from untreated uPA/SCID livers were not amplified by the primer set used for canine FIX and GAPDH detection (Fig. 3A).

Proliferation of FIX-producing human hepatocytes in uPA/SCID mouse livers

Human hepatocytes were transplanted into the liver of uPA/SCID mice (n=12). The proliferation and propagation status of the transplanted hepatocytes were assessed by periodic measurement of human albumin levels in the recipient blood, and the repopulation rate of human hepatocytes in the uPA/SCID livers was assessed as described previously (35, 38). Human FIX:Ag was detected in the plasma of 75% of the mice (9 out of 12) between 67 and 84 days after transplantation, and the circulating plasma levels ranged between 6–58% found in normal humans. The results from our study demonstrated that the FIX:Ag levels were highly correlated with the human albumin levels (R^2=0.8714) (Fig. 4A). To examine the biological function of the secreted human FIX, we compared the repopulation rate with FIX:C assays (Fig. 4B). Although both murine and human FIX:C could be measured using the clotting assay, we were able to estimate the approximate levels of the *de novo* expressed human FIX:C present in our samples. Plasma levels of FIX:C in untreated uPA/SCID mice were less than 50% of the levels normally found in human plasma, and we expected to increase the FIX:C levels up to 100% following the humanization of the murine livers. Similar to the canine transplants, the results showed that mice with a high repopulation rate had higher FIX:C than those with low repopulation rates (R^2=0.7245). These data suggested that secreted human FIX protein was biologically active. To clarify the proliferation status of transplanted human hepatocytes in uPA/SCID mouse liver, we also transplanted human hepatocytes isolated from another human subject (a 2-year-old Caucasian male) into a new set of uPA/SCID mice (n=9). Using these mice, we measured plasma human FIX:Ag levels, total plasma FIX:C levels, and human plasma albumin concentrations from samples obtained periodically from the recipient mice during an eight-week period after transplantation. As shown in Fig-

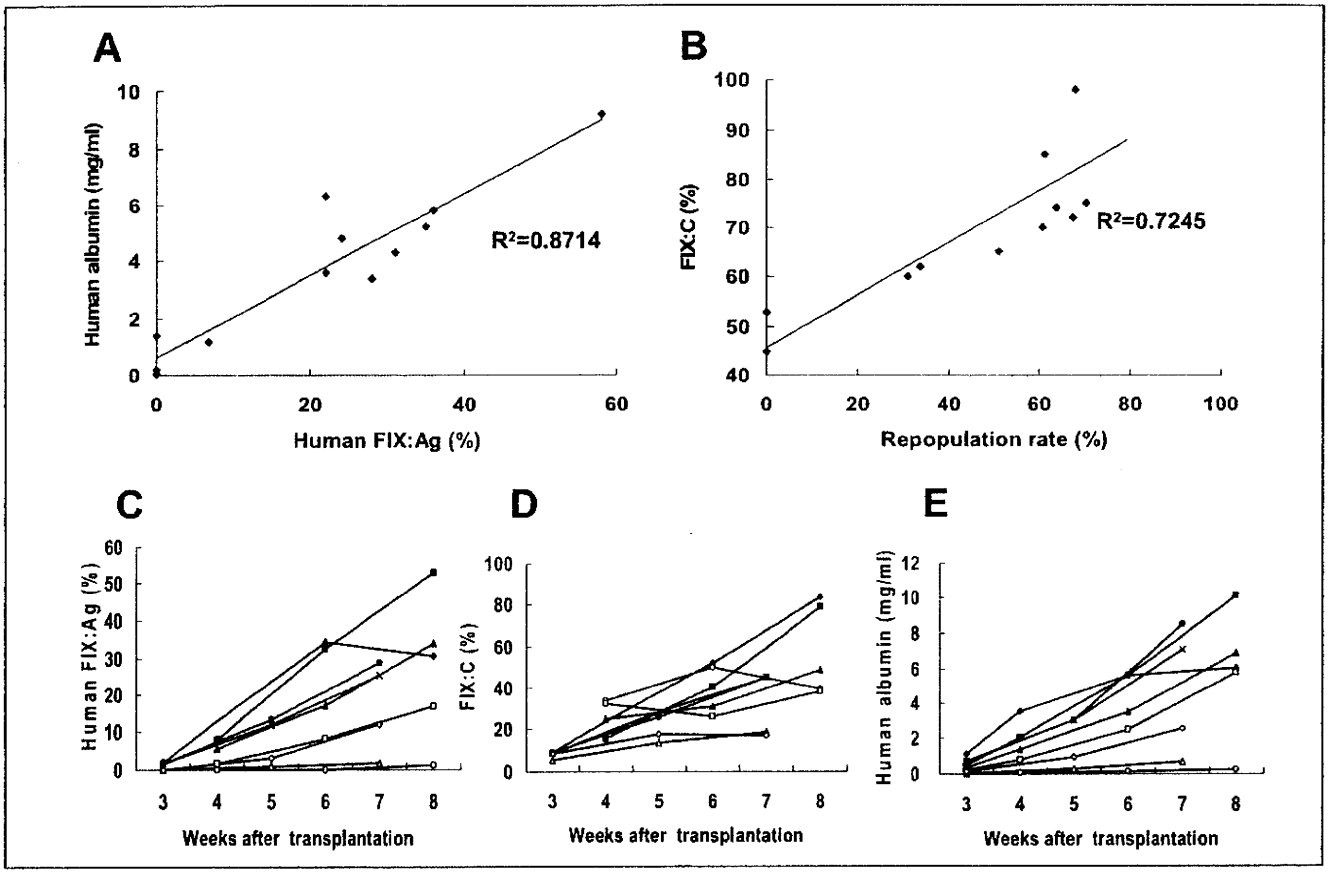

Figure 4: Proliferation of transplanted human hepatocytes in uPA/SCID mouse livers assessed by recipient blood analyses. A) Relationship between blood human albumin and plasma human factor IX (FIX) antigen (hFIX:Ag) concentrations of uPA/SCID mice transplanted with human hepatocytes (n=12). B) Relationship between total plasma FIX coagulation activity (FIX:C; reflecting both murine and human FIX activities) (% of normal human plasma) in uPA/SCID mice transplanted with human hepatocytes based on the repopulation rate estimated from human albumin concentrations as described in *Materials and methods*. The recipient blood samples used for these assays were obtained 67–84 days after transplantation. C-E) Time course of plasma hFIX:Ag levels (C), total plasma FIX:C levels (D), and blood human albumin levels (E) of the recipient mice after human hepatocyte transplantation (n=9) (different set of experimental data from that shown in A and B).

ure 4C-E, each of our measured parameters were found to be increased after transplantation in most of the mice, which was indicative of a robust proliferative status of the transplanted human hepatocytes.

Liver sections obtained from mice with high plasma human FIX:Ag levels were found to have strong positive staining in the hepatocytes for human FIX as determined by immunohistochemistry (Fig. 5B). In marked contrast, only a small portion of the liver stained positive in sections of recipient mice that were detected to have low (i.e. <1%) circulating levels of plasma FIX:Ag level (Fig. 5A). These results were consistent with the findings that the *de novo* production of haemostatically active human FIX in the circulation was dependent on the viability and persistence of the transplanted hepatocytes in the recipient uPA/SCID livers.

The uPA/SCID mice that received human hepatocytes were divided into three groups according to the repopulation rate (low <40%, medium 41–65%, and high >66%). Human FIX mRNA levels were normalized using glyceraldehyde-3-phosphate dehydrogenase (GAPDH) mRNA measurements (FIX:GAPDH). As shown in Figure 3B, the ratio of human FIX:GAPDH mRNA expression in the recipient livers was not significantly different among the three groups. We further confirmed that extracted total RNA from untreated uPA/SCID livers were not amplified by the primer set used for human FIX and human GAPDH detection (Fig. 3B), demonstrating the specificity of the primers to human and not murine FIX expression. Similar findings were determined in the canine hepatocyte transplantation experiments in which we confirmed that human hepatocytes proliferated in uPA/SCID mouse livers and retained their ability for transcribing the human FIX gene.

It has been reported that differentiated liver function (e.g. mRNA expression of albumin) may be suppressed when hepatocytes are subjected to various proliferative stimuli (40, 41). It is not known, however, if hepatocyte proliferation could directly influence FIX mRNA expression. To address this question, we compared FIX mRNA expression in quiescent and proliferating mouse livers. Liver proliferation was induced by performing a

70% hepatectomy in C57/BL6 wild-type mice, and the remnant liver lobes were subsequently harvested two days after the hepatectomy, which is the time point where hepatocyte proliferation is at its peak. The quiescent (non-proliferative) liver samples used in these experiments were the resected liver lobes obtained from the same mice in which the partial hepatectomy was performed. The relative FIX mRNA expression (FIX:GAPDH) was ~35% lower in the proliferating liver compared to the quiescent liver ($p=0.029$; Fig. 6). These results would suggest that the proliferative status of the transplanted hepatocytes may affect the production of FIX, and the reason for the lower FIX mRNA expression found in the recipient mice compared to the control livers as shown in Figure 3 may be due to active proliferation by the transplanted hepatocytes. If the FIX mRNA expression levels found in the normal canine and human livers were recalculated to account for a 35% reduction in response to proliferative stimuli, the significant differences between the four groups shown in Figure 3 became non-significant (data not shown). This suggests that proliferating hepatocytes in uPA/SCID mice have the capability of expressing normal levels of canine and human FIX following transplantation.

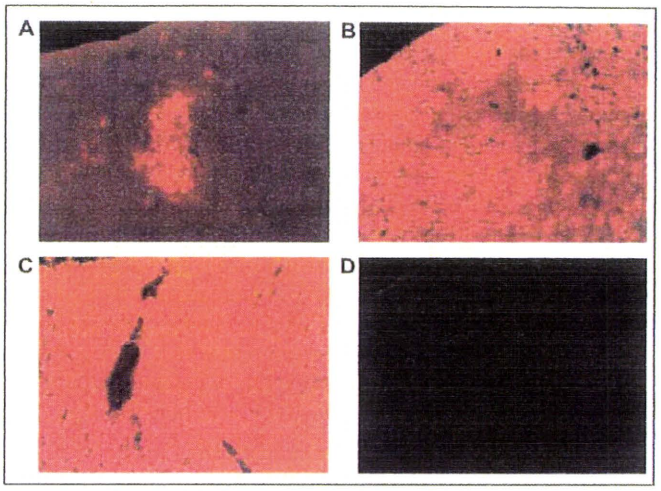

Figure 5: Mouse liver chimerism with proliferated human hepatocytes. Immunofluorecent staining of human FIX in liver sections of uPA/SCID mice after human hepatocyte transplantation. Liver sections of mice with <1% plasma hFIX:Ag level (A) and mice with 34% hFIX:Ag plasma level (B). Red-stained area indicates proliferated human hepatocytes producing hFIX. Positive control (normal human liver tissue) (C) and negative control (non-transplanted uPA/SCID mouse liver) (D) indicate the staining specificity for human FIX. Original magnification, ×100.

Discussion

We have established an *in vivo* system to propagate human and canine hepatocytes in uPA/SCID mouse livers, and these transplanted hepatocytes are capable of retaining their cellular machinery to produce coagulation FIX. The capabilities of these propagating transplanted hepatocytes to synthesize FIX were confirmed by the expression of FIX mRNA, FIX-protein production and secretion, and its coagulation activity. The main reason we decided to study canine hepatocyte in addition to human hepatocytes for transplantation, is the availability of a pre-clinical large animal model for haemophilia B studies (42), which will be able to be used for proof-of-concept experiments.

Hepatocytes are the only cells that are known to synthesize FIX (18), and successful liver transplantation has resulted in restoration of normal coagulative properties in patients with haemophilia B (17). Although there are obvious benefits in surgically transplanting whole livers in haemophilic patients with critical life-threatening liver diseases such as chronic active hepatitis, this approach is likely not appropriate for most patients due to other obvious negative risks associated with this type of procedure. For this reason, the hepatocyte transplantation approach described in the current study, which is less invasive and requires fewer donor livers, may provide a viable alternative strategy to organ transplantation. Recent trials have highlighted successful application of hepatocyte transplantation in two patients with coagulation factor VII deficiency (31, 43). Following hepatocyte transplantation, both patients were found to have achieved significant and prolonged therapeutic benefit with a marked decrease in the infusion of exogenous recombinant factor VIIa due to episodic bleeding (44, 45).

We demonstrated that canine and human hepatocytes progressively proliferated and propagated in the recipient livers of uPA/SCID mice. Real-time PCR analysis at various stages of hepatocyte propagation showed that FIX mRNA expression per transplanted cell (per donor-specific GAPDH mRNA level) was stably maintained for the duration of the experiment. Plasma FIX:Ag levels were highly correlated with the propagation status of the transplanted hepatocytes as determined by the blood levels of canine and human albumin. Furthermore, the procoagulant function of the secreted canine and human FIX was confirmed by clotting assays. FIX:C increased from baseline levels (less than 50% of normal human plasma) to normal human or canine FIX:C levels (about 100% and 200%, respectively) as repopu-

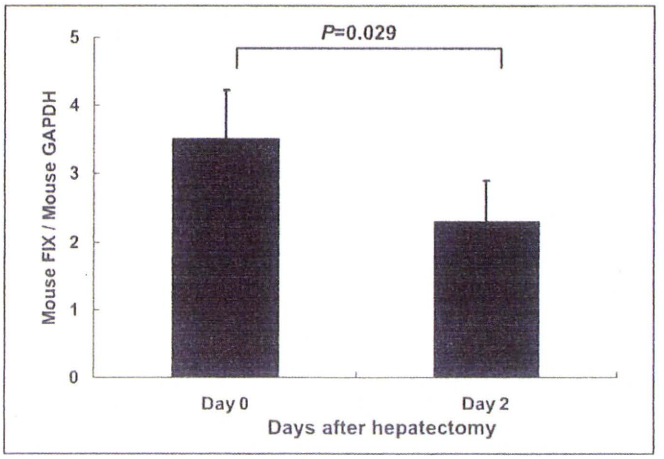

Figure 6: Comparison of factor IX (FIX) mRNA expression levels in quiescent and proliferating livers. Day 0 liver samples (quiescent status) were obtained from C57/BL6 mice at the time of 70% partial hepatectomy (n=6). The remnant liver lobes of the mice were harvested at day 2 were used for the assessment for proliferating status (n=6). Relative FIX mRNA expression was expressed as murine FIX / murine GAPDH.

lation by transplanted hepatocytes progressed. The data from our experiments indicated that post-transcriptional modification of FIX, including cleavage and removal of the pre-pro leader sequence of 46 amino-acids, γ-carboxylation of the first 12 glutamic acid residues, and partial β-hydroxylation of Asp 64 (46), must have occurred within the transplanted hepatocytes to maintain biologically active haemostatic function.

Hepatocytes from a one-year-old dog demonstrated high proliferation activity compared with cells from an older (7-year-old) dog as evidenced by the more rapid increase and its higher sustained levels of plasma canine FIX:Ag. These results are consistent with earlier findings by our group in which we reported that human hepatocytes from a younger donor occupied a larger proportion in the recipient uPA/SCID mouse liver compared with transplanted hepatocytes from an older donor (47). One possible reason for the enhanced growth potential of hepatocytes in these circumstances may be due to an elevated expression of cell cycle proteins in hepatocytes from younger compared to older donors (48). With the present study as well as previous work in the literature, we believe that the age of the donor makes a difference on the proliferation and repopulation of the transplanted hepatocytes in uPA/SCID mouse livers.

Human hepatocytes propagated in uPA/SCID mice could be isolated and purified using cell-sorting technology (38). Recently, our group has developed a procedure to isolate human hepatocytes that were propagated in uPA/SCID mouse livers, and these isolated hepatocytes were confirmed to be biologically functional compared to original primary hepatocytes, demonstrating the expression of cytochrome P450 (CYP) (38). We have also been experimentally successful in engineering functional liver tissue using isolated hepatocytes transplanted under the kidney capsule or in the subcutaneous space by demonstrating coagulation factor VIII expression (25–30). More recently, Azuma et al. (49) reported an alternate method to propagate human hepatocytes in living mice that furthers the utility of hepatocyte transplantation. Based on these developments, propagated human hepatocytes with FIX expressions should become a valuable cell source in establishing novel cell-based therapies for direct transplantation or development of tissue engineering strategies in the treatment of haemophilia B.

For the eventual translation of cell-based therapies using the propagated human hepatocytes for haemophilia B to be successful in the clinics, several potential obstacles will need to be considered and overcome. First, contamination of murine cells during the isolation of the transplanted human hepatocytes must be minimized. Second, increasing the engraftment rate of the transplanted hepatocytes into the recipient liver. Lastly, the survival and viability of the transplanted allergenic hepatocytes must be prolonged. With regards to the first issue, the contaminating murine hepatocytes during the isolation of human cells from the mouse liver could be overcome by utilizing recipient transgenic mice that have been incorporated with a inducible suicide gene. In the presence of the inducing agent, the murine cells would be preferentially eliminated and increase the purity of the human hepatocyte mixture leading to enhanced clinical safety. To overcome the low engraftment rate found in the current and previous studies, the recipient livers will require some type of preconditioning regimen to maximize the efficiency and engraftment. Slehria et al. (50) reported an effective and non-invasive pretreatment protocol in which the administration of phentolamine, an adrenergic receptor blocker, resulted in the dilation of the hepatic sinusoidal vasculature leading to enhanced hepatocyte engraftment rate. For the last issue regarding the limited graft survivability of the donor cells due to the activation of the host immune system, it will be important to design an immunosuppressive regimen specific for hepatocyte transplantation and monitoring systems for the early rejection need be established. These issues will need to be studied and overcome to substantiate the utility of this approach for the treatment of haemophilia and other congenital liver disorders.

In all, the present study has demonstrated the utility of hepatocyte transplantation for the therapeutic production of coagulation factor IX. As we continue to overcome the obstacles associated with this approach, this transplantation methodology will evolve into a novel approach to treat not only liver diseases associated with haemophilia but other forms of congenital liver diseases.

Acknowledgements

The authors thank Takeo Nomi and Eiji Okano (Department of Surgery, Nara Medical University) and Yuichi Komai (Department of Paediatrics, Nara Medical University) for their technical assistance with isolating canine hepatocytes, Jun-ichi Ori (Ori Animal Hospital, Osaka, Japan) for providing pooled normal canine plasma, Yoshihiko Sakurai and Keiji Nogami (Department of Paediatrics, Nara Medical University) for statistical advice, John C. Giddings (Department of Haematology, University of Wales College of Medicine) and Frank Park (Medical College of Wisconsin) for their critical reading of the manuscript, and Hiromi Kohno and Chihiro Yamazaki (Yoshizato Project, CLUSTER, Hiroshima Prefectural Institute of Industrial Science and Technology) for breeding and managing the uPA/SCID mice.

References

1. Bolton-Maggs PH, Pasi KJ. Haemophilias A and B. Lancet 2003; 361: 1801–1809.
2. Hsu TC, Nakaya SM, Thompson AR. Severe haemophilia B due to a 6 kb factor IX gene deletion including exon 4: non-homologous recombination associated with a shortened transcript from whole blood. Thromb Haemost 2007; 97: 176–180.
3. Nathwani AC, Davidoff AM, Tuddenham EG. Prospects for gene therapy of haemophilia. Haemophilia 2004; 10: 309–318.
4. Ehrhardt A, Kay MA. A new adenoviral helper-dependent vector results in long-term therapeutic levels of human coagulation factor IX at low doses in vivo. Blood 2002; 99: 3923–3930.
5. Herzog RW, Yang EY, Couto LB, et al. Long-term correction of canine hemophilia B by gene transfer of blood coagulation factor IX mediated by adeno-associated viral vector. Nat Med 1999; 5: 56–63.
6. Kay MA, Rothenberg S, Landen CN, et al. In vivo gene therapy of hemophilia B: sustained partial correction in factor IX-deficient dogs. Science 1993; 262: 117–119.
7. Miao CH, Thompson AR, Loeb K, et al. Long-term and therapeutic-level hepatic gene expression of human factor IX after naked plasmid transfer in vivo. Mol Ther 2001; 3: 947–957.
8. Mount JD, Herzog RW, Tillson DM, et al. Sustained phenotypic correction of hemophilia B dogs with a factor IX null mutation by liver-directed gene therapy. Blood 2002; 99: 2670–2676.
9. Nathwani AC, Davidoff A, Hanawa H, et al. Factors influencing in vivo transduction by recombinant adeno-associated viral vectors expressing the human factor IX cDNA. Blood 2001; 97: 1258–1265.